Accepted Manuscript

Circulating Peroxiredoxin-1 is a novel damage-associated molecular pattern and aggravates acute liver injury via promoting inflammation

Ying He, Shenglan Li, Damu Tang, Yu Peng, Jie Meng, Shifang Peng, Zhenghao Deng, Sisi Qiu, Xiaohua Liao, Haihua Chen, Sha Tu, Lijian Tao, Zhangzhe Peng, Huixiang Yang

PII: S0891-5849(18)32416-X

DOI: https://doi.org/10.1016/j.freeradbiomed.2019.04.012

Reference: FRB 14235

To appear in: *Free Radical Biology and Medicine*

Received Date: 23 November 2018

Revised Date: 14 March 2019

Accepted Date: 10 April 2019

Please cite this article as: Y. He, S. Li, D. Tang, Y. Peng, J. Meng, S. Peng, Z. Deng, S. Qiu, X. Liao, H. Chen, S. Tu, L. Tao, Z. Peng, H. Yang, Circulating Peroxiredoxin-1 is a novel damage-associated molecular pattern and aggravates acute liver injury via promoting inflammation, *Free Radical Biology and Medicine* (2019), doi: https://doi.org/10.1016/j.freeradbiomed.2019.04.012.

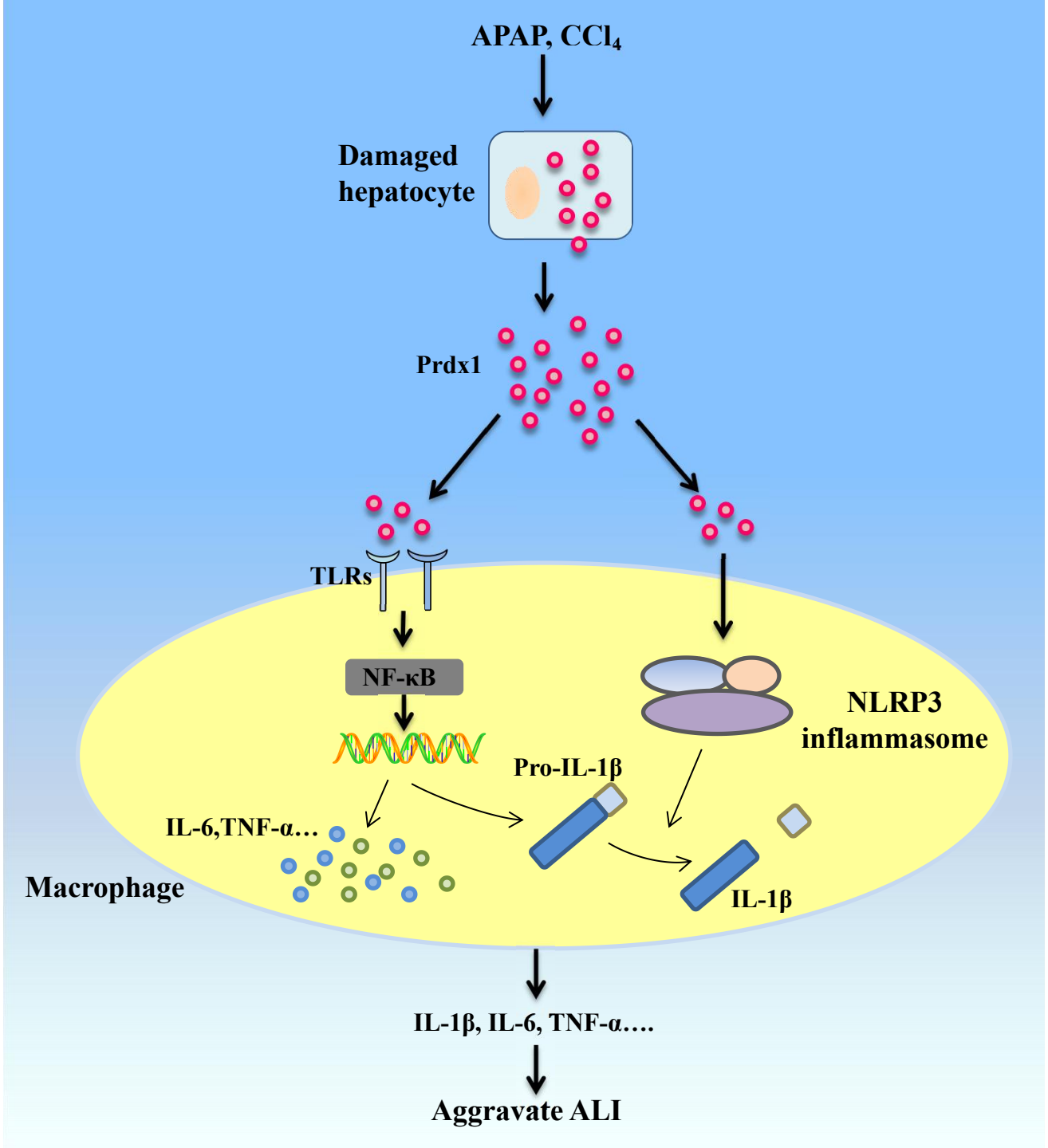
APAP, CCl_4
Damaged hepatocyte
Prdx1
TLRs
NF-κB
NLRP3 inflammasome
Pro-IL-1β
IL-6,TNF-α…
Macrophage
IL-1β
IL-1β, IL-6, TNF-α….
Aggravate ALI

Circulating Peroxiredoxin-1 is a Novel Damage-associated Molecular Pattern and Aggravates Acute Liver Injury via Promoting Inflammation

Ying He[1], Shenglan Li[1], Damu Tang[2], Yu Peng[1], Jie Meng[3], Shifang Peng[4], Zhenghao Deng[5], Sisi Qiu[1], Xiaohua Liao[6], Haihua Chen[1], Sha Tu[1], Lijian Tao[6], Zhangzhe Peng[6,*] and Huixiang Yang[1,*]

[1]*Department of Gastroenterology, Xiangya Hospital, Central South University, Changsha Hunan, China*
[2]*Hamilton Urologic Oncology Research Center (HUORC), St Joseph's Hospital* and *Department of Medicine, McMaster University, Hamilton, Ontario, Canada*
[3]*Department of Respiratory Medicine, Xiangya Hospital, Central South University, Changsha Hunan, China*
[4]*Department of Infectious Diseases, Xiangya Hospital, Central South University, Changsha Hunan, China*
[5]*Department of Pathology, Xiangya Hospital, Central South University, Changsha Hunan, China*
[6]*Department of Nephrology, Xiangya Hospital, Central South University, Changsha Hunan, China*

*Co-corresponding author

Huixiang Yang, Ph.D.
Department of Gastroenterology
Xiangya Hospital, Central South University
87 Xiangya Road, Changsha, Hunan 410008
China
Tel.: 86 731 84327106
Fax: 86 731 88879602
E-mail:yang_hx430@163.com

Zhangzhe Peng, Ph.D.
Department of Nephrology
Xiangya Hospital, Central South University
87 Xiangya Road, Changsha, Hunan 410008
China
Tel.: 86 731 84805215
Fax: 86 731 84805215
E-mail: pengzhangzhe@csu.edu.cn

Abbreviations

ALI: acute liver injury; ALT: alanine aminotransferase; APAP: acetaminophen; AST: aspartate aminotransferase; CCl_4: carbon tetrachloride; DAMPs: damage-associated molecular patterns; HMGB-1: high-mobility group protein B-1; IL-1β: interleukin-lβ; IL-6: interleukin-6; NF-κB: nuclear factor of kappa B; NLRP3: NOD-like receptor family pyrin domain containing 3; Prdx1: Peroxiredoxin-1; PRRs: pattern recognition receptors; rPrdx1: recombinant Peroxiredoxin-1; TBIL: total bilirubin; TLRs: Toll-like receptors; TNF-α: tumor necrosis factor-α.

Abstract

Sterile inflammation is initiated by damage-associated molecular patterns (DAMPs) and a key contributor to acute liver injury (ALI). However, the current knowledge on those DAMPs that activate hepatic inflammation under ALI remains incomplete. We report here that circulating peroxiredoxin-1 (Prdx1) is a novel DAMP for ALI. Intraperitoneal injection of acetaminophen (APAP) elicited a progressive course of ALI in mice, which was developed from 12 to 24 hours post injection along with liver inflammation evident by macrophage infiltration and upregulations of cytokines (IL-1β, IL-6 and TNF-α); these alterations were concurrently occurred with a robust and progressive production of serum Prdx1. Similar observations were also obtained in carbon tetrachloride (CCl_4)-induced ALI in mice. Removal of the source of serum Prdx1 protected mice deficient in Prdx1 from APAP and CCl_4-induced liver injury, and decreased macrophage infiltration, IL-1β, IL-6 and TNF-α production. As a result, *Prdx1*$^{-/-}$ mice were strongly protected from APAP-induced death that was likely progressed from ALI. Additionally, intravenous re-introduction of recombinant Prdx1 (rPrdx1) in *Prdx1*$^{-/-}$ mice reversed or reduced all the above events, demonstrating an important contribution of circulating Prdx1 to ALI. rPrdx1 potently induced in primary macrophages the expression of pro-IL-1β, IL-6, TNF-α, and IL-1β through the NF-κB signaling as well as the NOD-like receptor family pyrin domain containing 3 (NLRP3) inflammasome signaling, evident by caspase-1 activation. Furthermore, a significant elevation of serum Prdx1 was demonstrated in patients (n=15) with ALI; the elevation is associated with ALI severity. Collectively, we provide the first demonstration for serum Prdx1 contributing to ALI.

Keywords

Peroxiredoxin-1; acute liver injury; DAMPs; inflammation; NLRP3

1. Introduction

Acute liver injury (ALI) is mainly caused by hepatotoxic drugs, toxins and viral infection [1,2]. Hepatoxicity is the leading cause for drug withdrawal during development. ALI remains a major health issue; it can progress to liver failure and life-threatening conditions with little effective treatment. While the etiology underlying ALI remains incompletely understood, evidence supports a major role of damage-associated molecular patterns (DAMPs) in the disease pathogenesis [3-9]. DAMPs are molecules or signals released from damaged cells [10-14]; liver injury produces DAMPs which induce hepatic sterile inflammation via activating immune cells expressing pattern recognition receptors (PRRs) [9,15], including toll-like receptors and the NOD-like receptor family pyrin domain containing 3 (NLRP3), which leads to the production of inflammatory cytokines (IL-1β, IL-6 and TNF-α). Although much progress has been made in the understanding of sterile inflammation-contributed ALI, the role of specific DAMPs in ALI pathogenesis and the underlying mechanisms remain poorly defined.

Peroxiredoxin-1 (Prdx1) is a small protein (23kD) in the Peroxiredoxins family [16,17]; the family consists of ubiquitously expressed enzymes that reduce peroxide levels [18]. Prdx1 was discovered twenty years ago, and is well-known for its protective roles in many diseases such as aging, neurodegenerative diseases and cancers via anti-oxidative capability [19-24]. The protection is widely regarded to be attributable to Prdx1-derived anti-oxidant activities. Surprisingly, a significant elevation of Prdx1 in serum of patients with non-small cell lung cancer was observed [25]; additionally, evidence indicates that intracellular Prdx1 is released to the extracellular space in response to stimuli including TGF-β1, LPS and TNF-α [26-28]. Unexpectedly, extracellular Prdx1 has recently been identified as a novel DAMP attributed to its pro-inflammatory property via

binding to Toll-like receptor (TLR) 2/4 [29,30]. Extracellular Prdx1 substantiates ischemia-reperfusion-induced brain injury [31].

ALI is associated with extensive hepatocyte damage and thus several DAMPs, including high-mobility group protein B-1 (HMGB-1) [32,33], mitochondrial DNA [34,35] and heat shock protein [36]. As Prdx1 is a novel DAMP, we thought that Prdx1 plays a role in facilitating ALI. This possibility is supported by the observations that Prdx1 was released into the circulation in ischemic brain injury [31,37] and acute lung injury [38,39] and that circulating Prdx1 functions as a DAMP in promoting inflammation under these acute tissue injures.

We report here a significant elevation of circulating Prdx1 in mice with ALI caused by acetaminophen (APAP) or carbon tetrachloride (CCl_4). Circulating Prdx1 induces inflammation in part through the production of pro-inflammatory cytokines (IL-1β, IL-6 and TNF-α) involving the NF-κB and NLRP3 inflammasome signaling. Furthermore, an increase in circulating Prdx1 was also detected in patients with ALI. Collectively, our research supports Prdx1 as a novel DAMP in the pathogenesis of ALI.

2. Materials and Methods

2.1. Human Subjects

This study was approved by the Ethics Committee of Xiangya Hospital, Central South University with consent for all patients. Serum samples from normal subjects and patients with ALI or liver cirrhosis were accordingly obtained. The inclusion criteria were defined as previously reported [40]. Briefly, patients with ALI were recruited based on the criteria: 1) alanine aminotransferase (ALT)

level ≥5× the upper limit of normal (ULN); 2) alkaline phosphatase level ≥2× the ULN or ALT level ≥3× the ULN accompanied by a total of bilirubin (TBIL) level ≥2× the ULN. Additional clinical characteristics are shown in Table 1-2.

2.2. Materials

APAP was purchased from Sangon Biotech (#A506808, Shanghai, China) and dissolved in 0.9% saline. CCl_4 was obtained from Aladdin (#C1120430, Shanghai, China) and dissolved in olive oil. NF-κB inhibitor BAY117082 (BAY, #S2913), LPS inhibitor Polymyxin B (PMB, #S1395) and NLRP3 inhibitor MCC950 (#S7809) were requested from Selleck (Shanghai, China). Human Prdx1 ELISA kit was provided by Abnova (#KA0536, Taipei City, Taiwan). Mouse Prdx1 ELISA kit was purchased from CUSABIO (#CSB-EL018653MO, Hubei, China). Mouse ELISA kits for IL-1β (#MLB00C), IL-6 (#M6000B) and TNF-α (#MTA00B) were purchased from R&D Systems (Minneapolis, USA).

Recombinant Prdx1 (rPrdx1) was obtained from Abnova (#P4543, Taipei City, Taiwan). The full-length rPrdx1 was generated by using an *Escherichia coli* expression system with purity more than 95% (http://www.abnova.com).

2.3. Mouse Models

Prdx1-knockout (*Prdx1*$^{-/-}$) C57BL/6J mice were generated in our laboratory using the CRISPR/Cas9 technique (Supplementary Fig.1). Eight to ten weeks old male *Prdx1*$^{-/-}$ and wild type (WT) mice were used. Animal care was provided in compliance with the Guidelines for the Care

and Use of Laboratory Animals published by the National Institutes of Health (NIH). Experimental protocols were approved by the Ethics Review Committee for Animal Experimentation of Central South University. Mice were maintained in SPF-class housing of laboratory under a 12-hour dark/12-hour light cycle with free access to food and water unless otherwise indicated.

APAP-induced ALI model was generated by intraperitoneal (i.p.) injection of APAP into WT and *Prdx1*$^{-/-}$ mice at a lethal dose (750mg/Kg) once and observed for 7 days. Animals were also injected with a sub-lethal dose (500mg/Kg) once and sacrificed 12 or 24 hours later.

CCl_4-induced ALI model was produced by i.p. injection of a CCl_4 mixture of olive oil: CCl_4 (3:1; 2ml/Kg) once and sacrificed after 2, 4 or 7 days.

CCl_4-induced model for chronic liver injury was obtained through i.p. injection of the CCl_4 mixture at 2ml/Kg twice a week for 4, 6 or 8 weeks.

2.4. Histological and Immunohistochemical Analysis

Mouse liver tissue specimens were fixed in 4% neutral buffered formalin, and embedded in paraffin. The paraffin-embedded sections (4μm) were stained with hematoxylin and eosin (H&E), Masson's trichrome or Sirius red, as previously described [41]. For the immunohistochemical analysis of Prdx1 (#ab15571, Abcam, Cambridge, UK) and F4/80 (#CI-A3-1, Novus Biologicals, Minneapolis, USA) expression, endogenous peroxidase activity was blocked for 20 min, and the tissues were subjected to antigen retrieval with 6.5 mM citrate buffer (pH 6.0) for 15 min in a microwave, after which the slides were incubated with a primary antibody (1:200 for Prdx1, 1:100 for F4/80) overnight at 4°C. After immunostaining for DAB, the sections were counterstained with hematoxylin. Two independent pathologists blindly performed histological assessments.

2.5. Assessment of Liver Function

Liver function was evaluated using blood samples from each mouse at the end of the experiment duration. Liver function measurements were performed using theAU680 Chemistry System (Beckman Coulter Inc., USA) in the clinical laboratory of Xiangya Hospital, Central South University.

2.6. Isolation and Culture of Primary Peritoneal Macrophages

Primary peritoneal macrophages were isolated from WT mice as previously described [42], and cultured in RPMI 1640 medium (Life Technologies, Grand Island, NY) supplemented with 10% fetal bovine serum (FBS), 100U/ml penicillin and100U/ml streptomycin at 37°C in an atmosphere of 5% CO_2. Primary peritoneal macrophages were pre-incubated with BAY (50μM), PMB, (10μg/ml) or MCC950 (10μM) for one hour and then exposed to recombinant Prdx1 (rPrdx1) for hours as designed.

2.7. Isolation and Culture of Primary Mouse Hepatocytes

Primary mouse hepatocytes were isolated from male C57BL/6J mice (aged8–10 weeks) by a non-reticulating perfusion of livers with 0.05% Collagenase Type IV (#C5138, Sigma, St Louis, MO). Hepatocytes were purified by repeated centrifugation at 50g and seeded in 12-well plates with Dulbecco's modified Eagle medium (DMEM) supplemented with 10% FBS, 100U/ml penicillin

and 100U/ml streptomycin at 37°C in a humidified atmosphere of 5% CO_2 overnight. Hepatocytes were then incubated in FBS-free medium and treated with or without different doses of APAP for 6-24 hours. The culture mediums were collected to measure the released Prdx1 by an ELISA kit according to the manufacturer's instructions. Experiments using primary hepatocytes were performed 24 to 48 hours after isolation and harvested within 72 hours.

2.8. ELISA and Measurement of MDA

Serum and cellular supernatant levels of Prdx1, IL-β, IL-6, and TNF-α were measured by ELISA kits. Serum malondialdehyde (MDA) level was detected by TBARS kit from R&D Systems (#KGE013, Minneapolis, USA). These experiments were performed according to the manufacturer's instructions.

2.9. Western-blotting Analysis

Protein extracted from fresh liver tissues or cultured cells were separated on 10-12% SDS-polyacrylamide gels and then transferred onto polyvinylidene difluoride membranes (Millipore, Darmstadt, Germany), which were incubated with antibodies against Prdx1 (1:5000, #ab15571, Abcam, Cambridge, UK), NLRP3 (1:1000, #AG-20B-0014, Adipogen, San Diego, USA), pro-IL-1β (1:800, #sc-7884, Santa Cruz, Dallas, USA), IL-1β (1:800, #sc-7884, Santa Cruz, Dallas, USA), pro-caspase-1 (1:500, #sc-56036, Santa Cruz, Dallas, USA), caspase-1 (1:500, #sc-56036,Santa Cruz, Dallas, USA) and GAPDH (1:5000, #G9295, Sigma-Aldrich, Darmstadt, Germany) overnight at 4°C before being hybridized with HRP-conjugated secondary antibodies for

1 hour at room temperature. The bands were visualized by an ECL kit and quantified with BandScan 5.0 Software (Glyko, Novato, CA). The full-length and cleaved forms of the proteins were distinguished by molecular weight [43]: pro-IL-1β is 31kD, IL-1β is 17kD; pro-caspase-1 is 45kD, caspase-1 is 10kD.

2.10. Analysis of mRNA Expression

Real-time PCR analysis was performed as previously described [44]. Total RNA were isolated from liver tissues using TRIzol reagent according to the manufacturer's instructions. First-strand cDNA was synthesized from 2μg of total RNA in a 20μl reaction using reverse transcriptase (Fermentas, MD). The specific primers for *Prdx1-6*, inflammatory cytokines (*IL-1β, IL-6, TNF-α)* and *β-actin* (Supplementary Table 1) were synthesized by Sangon Biotech (Shanghai, China). The expression levels of specific mRNAs in each sample were calculated from the standard curve and normalized to β-actin mRNA expression. The comparative $2^{-\triangle\triangle CT}$ method was used for quantification and statistical analysis.

2.11. Statistical Analysis

All data are expressed as the mean±SD. Statistical analysis was performed with SPSS 22.0 software (SPSS, Chicago, IL). Comparisons between groups were made with one-way ANOVA, and linear correlations were analyzed by Pearson's correlation coefficient. The Kaplan–Meier method was used to assess the differences in survival between the groups. $P<0.05$ was considered statistically significant.

3. Results

3.1. A significant elevation of circulating Prdx1in mice with ALI induced by APAP or CCl_4

An increase in circulating Prdx1 was previously detected in mice with ischemic brain injury [45] and acute lung injury [39]; the released extracellular Prdx1 functioned as a DAMP by inducing sterile inflammation and thus contributed to the tissue injuries [29,31,37,38,46]. These observations suggest a potential contribution of circulating Prdx1 to ALI. APAP is a common drug causing ALI in humans [47] and has been widely used in studies for drug-induced ALI in mice. To investigate a potential production of Prdx1 in the circulation of mice with ALI, we have i.p. injected APAP (500mg/Kg) into C57/BL6 mice and examined liver injury 12 or 24 hours later. Liver injury occurred at 12 hours post injection (Fig 1A-C); severity of the injury progressed from 12 hours to 24 hours, evident by an increase of the region with centrilobular necrosis (Fig1A) and an elevation of serum ALT (Fig1B) at 24 hours compared to 12 hours. The kinetics of liver damage caused by APAP injection in this study was comparable to APAP-induced liver injury reported by others [48,49]. Importantly, we detected a significant increase in serum Prdx1 in mice at 12 hours following APAP injection, which was further increased at the 24 time point (Fig 1D).

To further support the upregulation of serum Prdx1 in mice with ALI, we have induced liver damage in C57/BL6 mice by one time i.p. injection of CCl_4 (2ml/Kg) and examined liver injury in a period of 2, 4, and 7 days. A transient liver injury was evident at day 2 based on increases in hepatocyte necrosis (Fig 1E), serum ALT (Fig 1F), and serum AST (Fig 1G), which was followed by a recovery phase from day 4 onward (Fig 1E-G). These results are in accordance with the

knowledge that CCl_4 in an acute setting caused ALI, which was healed subsequently [50,51]. As observed in mice with ALI induced by APAP, a significant increase in circulating Prdx1 was detected in CCl_4-treated mice with liver damage but not in those recovered (Fig 1H). APAP and CCl_4 induce ALI with different mechanisms [52]; the detection of serum Prdx1 in two different mouse models for ALI strongly suggests its general involvement in ALI. This concept is further supported by the lack of an elevation of circulating Prdx1 in mice with chronic administration of CCl_4 twice per week for 8 weeks (Supplementary Fig 2).

3.2. Serum Prdx1 contributes to ALI

The common detection of serum Prdx1 in ALI caused by different mechanisms (Fig 1D, H) indicates circulating Prdx1 being physiologically relevant to ALI. This potential functionality can be tested using a neutralization antibody to serum Prdx1. However, this reagent is not currently available. We thus took a genetic approach to address this issue. A mouse line deficient in Prdx1 was generated using the CRISPR-Cas9 technology. *Prdx1*$^{-/-}$ mice do not express Prdx1 in multiple organs examined, including the liver (Supplementary Fig 1). *Prdx1*$^{-/-}$ mice are viable, fertile, and healthy at age at least up to 8 months, which is consistent with the reported anemia development in aging *Prdx1*$^{-/-}$ mice (9 months and older) [24].

With the availability of *Prdx1*$^{-/-}$ mice, we determined the impact of Prdx1 on ALI. *Prdx1*$^{-/-}$ male (8-10 weeks old) and age-matched C57/BL6 mice were induced for ALI by one time i.p. injection of APAP (500 mg/Kg), and observed at 12 hours and 24 hours post injection. In comparison to C57/BL6 mice, *Prdx1*$^{-/-}$ mice displayed less hepatocyte necrosis (Fig 2A), and reduced the levels for all liver damage indicators examined: serum ALT (Fig 2B), serum aspartate aminotransferase (AST)

(Fig 2C), TBIL (Fig 2D), and direct bilirubin (DBIL, Fig 2E) at both 12 and 24 hours post injection. *Prdx1*$^{-/-}$ mice were also protected from CCl_4-induced ALI, evident by significantly decreases in hepatocyte necrosis, serum ALT, serum AST, and TBIL in *Prdx1*$^{-/-}$ mice at 2 days following CCl_4 injection (Fig 3A-E). While the protection remains incomplete, the fact that the protection occurred in *Prdx1*$^{-/-}$ mice subjected to ALI by different mechanisms (APAP and CCl_4) along with dramatic upregulations of circulating Prdx1 under these ALI conditions support a general role of serum Prdx1 in promoting ALI. This protection was unlikely due to possible compensations by other members of Prdxs which might be resulted from Prdx1 deficiency, as Prdx2, Prdx3, Prdx4, Prdx5, and Prdx6 were expressed at comparable levels in WT and *Prdx1*$^{-/-}$ mice (Supplementary Fig 3).

To further examine the above concept, we have investigated the effects of Prdx1 deficiency on chronic liver damage induced by CCl_4. Unlike in the CCl_4-induced ALI model in which hepatocyte necrosis occurred (Fig 1E), persistent administration of CCl_4 in C57/BL6 mice caused extracellular matrix deposition, revealed by increases in hepatic Masson staining (Supplementary Fig 4A), and induced liver fibrosis, evident by elevations in fibrotic score (Supplementary Fig 4B). Additionally, in this experimental duration, prolonged CCl_4 administration did not elicit significant liver damage in C57/BL6 mice based on the serum levels of ALT and AST (Supplementary Fig 4C). Interestingly, knockout of Prdx1 did not affect all aforementioned events (Supplementary Fig 4A-C). Collectively, the observed specificity of Prdx1 in facilitating ALI but not chronic liver injury is in line with a general involvement of serum Prdx1 in ALI.

3.3. Characterization of serum Prdx1-derived promotion of ALI

To directly study whether the protection in *Prdx1*$^{-/-}$ mice was attributable to the lack of circulating

Prdx1, we obtained rPrdx1 from Abnova (Taipei City, Taiwan) according to previous report [53]. *Prdx1*$^{-/-}$ mice were subsequently induced for ALI by APAP using the 24 hour-setting in the presence and absence of rPrdx1 (200 ng/mouse); vehicle (PBS) and rPrdx1 were intravenously delivered following i.p. injection of APAP. The use of rPrdx1 at dose of 200 ng/mouse rPrdx1 was based on several considerations; 1) the maximal level of serum Prdx1 detected in APAP-treated mice was approximately 30 ng/ml (Fig 1D); 2) mice have approximately 58.5 ml blood/kg on average (https://www.google.com/search, search term: mouse blood volume ml/kg); 3) for 8-10 weeks old males with an average 1.5 ml blood (25g/1000 x 58.5), 200 ng rPrdx1 was equivalent to 133 ng/ml, which was 4.4 (133/30) fold of endogenous circulating Prdx1; 4) it was likely that rPrdx1 was not as active as endogenous circulating Prdx1, 200 ng/ml rPrdx1 was likely within a physiological range; and 5) this dose could produce the maximal impact on the survival of *Prdx1*$^{-/-}$ mice on APAP-derived toxicity (see section 3.6 for details). Compared to the vehicle control, serum rPrdx1 significantly aggravated liver injury caused by APAP (Fig 4A-C). These observations demonstrated that the lack of circulating Prdx1 was responsible for the resistance of *Prdx1*$^{-/-}$ mice to APAP-induced liver injury.

Extracellular Prdx1 has been reported to be released from damaged brain cells and subsequently augmented brain injury via activation of sterile inflammation in the brain [31,37,54]. We have thus made an effort to examine whether circulating Prdx1 in mice with ALI was liver-origin. 1) Both APAP and CCl_4 are widely used to study liver toxicity, which supports the concept that the serum Prdx1 in mice treated with both drugs was resulted from damaged liver tissues. 2) Drug-induced ALI is primarily caused by hepatocyte damage [55-57]; in accordance with this knowledge, we were able to show that APAP dose-dependently induced primary mouse hepatocytes releasing Prdx1 into the extracellular space in an apparently efficient manner (Fig 5A, B). 3) Compared to normal

livers, livers with APAP-induced ALI showed a significant reduction of hepatic Prdx1 content and the level of reduction followed the development of ALI (Fig 5C-D). 4). In mice with a chronic liver disease caused by persistent treatment with CCl_4, the lack of damages in hepatocytes concurrently occurred with the lack of serum Prdx1 (Supplementary Fig 2). Collectively, these observations support the hepatic origin of serum Prdx1 in mice with ALI.

Prdx1 is well-known for its anti-oxidant activity that protects oxidative stress-caused diseases [18,20,58]. Oxidative stress is a pathogenic factor in ALI [59]. It is thus a possibility that liver-associated Prdx1 protects ALI by anti-oxidant activity, while liver-released Prdx1 promotes ALI. In this context, the loss of liver-associated Prdx1 observed in APAP-treated livers (Fig 5C-D) alone would aggravate oxidative stress during ALI pathogenesis. However, evidence does not support this possibility; both APAP and CCl_4 induced comparable levels of MDA (a maker of lipid peroxidation [60]) in *Prdx1*$^{-/-}$ mice and age-matched C57/BL6 mice (Supplementary Fig 5A, B). Furthermore, under the same conditions *Prdx1*$^{-/-}$ mice were protected from the drug-induced ALI compared to C57/BL6 mice (Figs 2, 3). Taken together, evidence supports that hepatic Prdx1 is a pro-ALI factor following its release into the circulation system independent of its anti-oxidant activity. This intriguing possibility is in line with cell-free Prdx1 as a DAMP without the involvement of its anti-oxidant enzymatic activity [29,31,61].

3.4. Association of circulating Prdx1 with inflammation in ALI

Circulating Prdx1 has been reported to function as a DAMP to augment acute brain ischemia-reperfusion injury and lung injury through activation of sterile inflammation [31,38]. Sterile inflammation is a well-demonstrated and major pathological factor of ALI [2,4,7,9],

suggesting that serum Prdx1 is associated with hepatic inflammation in ALI. To examine this association, we were able to show a significant and progressive increase in macrophage infiltration in livers of APAP-treated C57/BL6 mice following ALI progression, evident by an elevation in the number of F4/80-positive macrophages (Fig 6A; Supplementary Fig 6A). F4/80 is a biomarker of macrophages [62]. Consistent with macrophage infiltration, hepatic expression of IL-1β, IL-6, and TNF-α was also elevated in C57/BL6 mice in response to APAP (Fig 6B-D), demonstrating an-going inflammation in liver with ALI. More importantly, these hepatic inflammatory events were all significantly reduced in APAP-treated *Prdx1*$^{-/-}$ mice (Fig 6A-D; Supplementary Fig 6A), supporting a correlation of Prdx1 with sterile inflammation occurred in ALI. This concept is strengthened by the down-regulation of hepatic sterile inflammation in *Prdx1*$^{-/-}$ mice elicited by CCl_4 (Fig 6E-H; Supplementary Fig 6B).

The decreases in liver inflammation in *Prdx1*$^{-/-}$ mice treated with APAP were attributable at least in part to the lack of circulating Prdx1, as intravenous administration of rPrdx1 significantly increased hepatic macrophage infiltration as well as hepatic expression of IL-1β, IL-6, and TNF-α in *Prdx1*$^{-/-}$ mice treated with APAP (Fig 6I-L; Supplementary Fig 6C). Collectively, these results demonstrate an association of circulating Prdx1 with hepatic sterile inflammation in drug-induced ALI.

3.5. Prdx1 induces inflammatory cytokines production in primary peritoneal macrophages through the NF-κB and NLRP3 inflammsome signaling pathways

Our observed association of serum Prdx1 with macrophage infiltration and the production of aforementioned cytokines in livers undergoing ALI indicate a potential cytokine induction in

macrophages by extracellular Prdx1. This possibility is in accordance with macrophage being the major cell type contributing to inflammation in ALI [63-66]. To investigate this concept, we have isolated peritoneal macrophage from mouse and treated these cells with rPrdx1 in a range of doses. rPrdx1 clearly induced pro-IL-1β expression in primary macrophages in a dose-dependent manner (Fig 7A) and the induction by 25 nM rPrdx1 was within a linear range (Fig 7A). This condition was thus selected to characterize rPrdx1-mediated upregulation of inflammatory cytokines. At 25 nM, rPrdx1 induced the production of mature IL-6, mature TNF-α, and pro-IL-1β in primary macrophages in a time-dependent manner but with different kinetics (Fig 7B-D); within the induction duration (24 hours), the pro-IL-1β production was reached plateau between 3-6 hours, while mature IL-6 and TNF-α were continuously accumulated (Fig 7B-D).

In view of the major function of the NF-κB signaling in regulating cytokine expression [67,68] and considering the knowledge that rPrdx1 stimulates NF-κB activation [29,30,53,61]. We have determined a contribution of the NF-κB pathway in rPrdx1-stimulated expression of the above cytokines (Fig 7A-D). This small molecule inhibitor BAY 11-7082 at 50 μM has been widely used to inhibit NF-κB signaling [69,70]. At this condition, BAY 11-7082 robustly inhibited the expression of IL-6, TNF-α, and pro-IL-1β in primary macrophages treated with rPrdx1 (Fig 7B-D). The LPS inhibitor PMB did not affect the production of these cytokines, which eliminated the possibility that the observed effects by rPrdx1 was due to potential contamination of LPS with rPrdx1 (Fig 7B-D). Furthermore, heat treatment of rPrdx1 abolished its activity in inducing these cytokines (Fig 7B-C), indicating the heating condition has disturbed rPrdx1 structure or “pattern” required for cytokine inductions. These results collectively support a major role of the NF-κB pathway in facilitating rPrdx1-induced expression of the aforementioned cytokines.

Extracellular Prdx1 was reported to be a DAMP in the augmentation of

ischemia-reperfusion-induced brain injury [31,37]. A major effector for DAMPs to initiate sterile inflammation is the NLRP3 inflammasome complex [4,11,71], suggesting NLRP3 being involved in cell-free Prdx1-mediated inflammation. To investigate this possibility, we first examined the production of mature IL-1β, as maturation of IL-1β (cleavage of pro-IL-1β and secretion of IL-1β) depends on the NLRP3 inflammasome signaling [72]. rPrdx1 stimulated the production of mature IL-1β in primary macrophages starting from 12 hours, which was continuously produced at least up to 24 hours of Prdx1 stimulation (Fig 7E). The likelihood of structure alterations by the heat treatment robustly prevented rPrdx1 from inducing IL-1β maturation in primary macrophages (Fig 7E). As expected, BAY 11-7082 robustly inhibited IL-1β maturation in primary macrophages treated with rPrdx1 (Fig 7E), which was likely attributable to the inhibition of pro-IL-1β expression (Fig 7B). Importantly, blocking of the NLRP3 inflammasome signaling by MCC950 abolished the IL-1β production (Fig 7E), supporting the involvement of the NLRP3 inflammasome complex in rPrdx1-initiated sterile inflammation.

To further examine this possibility, we were able to show an upregulation of NLRP3 expression and caspase-1 activation in primary macrophages stimulated with rPrdx1 (Fig 7F). Interestingly, both events co-occurred with the production of mature IL-1β, i.e. they were started at 12 hours of rPrdx1 stimulation and proceeded to higher levels at 24 hours (Fig 7E, F). As the NLRP3 inflammasome complex is a platform for caspase-1 to cleave IL-1β and IL-18, a proteolytic step required for their maturation [73,74], the observations above thus support a feedback regulation in which rPrdx1 activates the NLRP3 inflammasome complex, which in turn mediates rPrdx1's actions in inducing IL-1β maturation. This feedback regulation depends on NF-κB signaling, as BAY 11-7082 abolished caspase-1 activation and NLRP3 expression in rPrdx1-treated primary macrophages (Fig 7F). On the other hand, the NLRP3 inhibitor MCC950 only suppressed

rPrdx1-induced caspase-1 activation but not NLRP3 upregulation (Fig 7F). Taken together, the above results revealed that rPrdx1 initiated a complex reaction in primary macrophages, leading to NLRP3 upregulation, caspase-1 activation, and the activation of the NLRP3 inflammasome complex.

3.6. Circulating Prdx1 contributes to poor outcomes in ALI

Acute liver injury can progress to poor outcomes: acute liver failure, liver transplantation, and fatality [75]. Our observed associations of serum Prdx1 with liver inflammation *in vivo* and rPrdx1-mediated robust induction of cytokine expression in primary macrophages *in vitro* suggest a role of circulating Prdx1 in promoting ALI progression. To examine this concept, we have induced *Prdx1*$^{-/-}$ (n=14) and age-matched C57/BL6 mice (n=14) with enhanced ALI through one time i.p. injection of APAP at 750 mg/kg and monitored the disease progression. C57/BL6 mice died at a significant faster kinetics compared to *Prdx1*$^{-/-}$ mice with 21.4% (3/14) and 42.8% (6/14) of death in WT mice vs 0% and 7.14% (1/14) of fatality in *Prdx1*$^{-/-}$ mice at 24 hours and 48 hours post injection respectively (p=0.0026) (Fig 8A). The protection observed in *Prdx1*$^{-/-}$ mice was at least in part attributable to the lack of serum Prdx1, evident by a significant sensitization of *Prdx1*$^{-/-}$ mice to APAP-derived toxicity upon intravenous injection of rPrdx1 (Fig 8B). At 10 μg/Kg which is equivalent to 200 ng/mouse, rPrdx1 achieved the maximal level of the sensitization (Fig 8B), which provided the rationale for using rPrdx1 at 200 ng/mouse to study its impact on ALI (Fig 4). Collectively, evidence supports serum Prdx1 as a contributing factor to ALI progression.

3.7. Elevation of circulating Prdx1 in patients with ALI

To further investigate the relevance of serum Prdx1 in ALI, we have organized a patient cohort consisting of normal subjects (n=15), patients with ALI (n=15), and patients with cirrhosis (n=15) (Table 1). Among 15 patients with ALI, 9 (60%) were caused by hepatitis B virus and 6 (40%) were drug-induced (Table 2). Except the significant lower level of TBIL and DBIL in patients with drug-induced ALI, there were no significant differences in other liver function tests in patients with ALI caused by either hepatitis B virus or drugs (Table 2). Importantly, circulating Prdx1 levels remained comparable in both types of ALI patients (Table 2). We thus ignored the etiology of ALI and used all ALI patients as a single entity in this analysis. Compared with normal subjects, a significant increase in circulating Prdx1 was observed in patients with ALI, but not in patients with liver cirrhosis (Fig 9A). Liver cirrhosis is a chronic disease which is mainly caused by deposition of extracellular matrix; these patients often have normal ALT and AST level. As an acute disease, damage in ALI occurs largely on hepatocytes [2,76,77]. No obvious alterations of serum Prdx1 in patients with cirrhosis over normal people indicate a specific increase in circulating Prdx1 in ALI. This concept is supported by an elevation of serum Prdx1 in patients with ALI in comparison to patients with cirrhosis (Fig 9A).

We subsequently attempted to examine whether serum Prdx1 has a predictive value towards ALI progression. Using our small cohort, a positive correlation between circulating Prdx1 and serum ALT (Fig 9B) or serum AST (Fig 9C) could be demonstrated, indicating an association of serum Prdx1 abundance with the severity of liver injury. In a recent investigation of 386 patients with ALI, bilirubin value was found of being the second most predictive factor of ALI progression [75]. Of note, serum Prdx1 in our study displays a significant positive correlation with serum TBIL (Fig 9D), supporting circulating Prdx1 as a biomarker of ALI.

4. Discussion

DAMPs are key initiators in inflammation exacerbating ALI. Due to lack of effective treatments, key mediating factors and pathogenesis of this disease need to be further explored. In this study, we provide the first demonstration for a specific elevation of circulating Prdx1 in APAP- and CCl_4-induced ALI in mice and patients with ALI; however, serum Prdx1 was not significantly altered in chronic liver injuries in either. More importantly, circulating Prdx1 contributes to ALI pathogenesis and progression.

We took multiple approaches to show circulating Prdx1 as a pathological factor of ALI. In mice deficient in Prdx1, both APAP and CCl_4 were significantly less potent in inducing ALI; the resistance was substantially reduced by restore of serum Prdx1 using rPrdx1. Furthermore, rPrdx1 was able to upregulate pro-IL-1β, IL-6 and TNF-α in primary macrophages through the NF-κB pathway; these observations are in accordance with previous reports for Prdx1-derived induction of inflammatory cytokines via activating the TLR2/4-NF-κB pathway [29,31]. Nonetheless, we provide the first evidence showing that rPrdx1 induces NLRP3 upregulation in primary mouse macrophages, which in a positive feedback manner facilitates rPrdx1-mediated activation of the NLRP3 inflammasome complex, resulting in caspase-1 activation and IL-1β maturation. Collectively, our research supports circulating Prdx1 as a novel DAMP to sustain ALI pathogenesis.

While the lack of circulating Prdx1 was protective to drug-induced ALI, the protection remains incomplete (Figs 2, 3); and ALI continuously progresses from 12 hours to 24 hours post APAP injection (Fig 2). The status of incomplete protection shows the involvement of other factors in ALI. These factors could include other DAMPs that are associated with ALI, such as HMGB-1 [32,33], mitochondrial DNA [34,35] and heat shock protein [36]. Additionally, other Prdxs members could

also act as DAMPs for ALI; for incidence, Prdx2 and Prdx5 were found in the extracellular space and contribute to ischemia-reperfusion-induced brain injury [31]. Whether either Prdxs or other members of Prdxs also function as DAMPs for ALI should be investigated in the future. Future research also needs to address the mechanisms underlying cell-free Prdx1-mediated activation of NF-κB and the NLRP3 inflammasome complex. 1) Is the enzyme activity of rPrdx1 required? 2) Which structural features are critical for rPrdx1 to activate the NF-κB and the NLRP3 inflammasome complex? 3) Will rPrdx1 function in this domain by binding unknown cellular proteins? 4) What are these proteins? 5) Will these cellular proteins stay inside or outside of macrophages? It can be envisaged that these investigations may lead to identification of cellular factors or unique structural elements of rPrdx1 which may have therapeutic potential in ALI management.

We have provided several lines of evidence suggesting the hepatic origin of serum Prdx1 in ALI (see section 3.3 for details). We realize that this issue needs be directly examined in the future. With the availability of *Prdx1*$^{-/-}$ mice, this issue could be examined by hepatocyte-specific reintroduction of Prdx1, and then examine APAP-mediated production of serum Prdx1. Alternatively, mice with liver-specific knockout of Prdx1 could also be used.

While the mechanisms responsible for releasing Prdx1 into the extracellular space are unclear, it is likely these mechanisms being complex. *Prdx1* is an inducible gene under stress conditions, especially during the acute inflammatory response [78,79]. Recently, several studies have observed the elevation of circulating Prdx1 in patients with ischemic brain injury [45,80] and cancers [20,23-25]. Stress is known to cause cells to release exosomes [81]. APAP has been shown to cause liver to release exosomes which was toxic to hepatocytes *in vitro* and recipient mice *in vivo* [49]. It is thus tempting to suggest that microvesicles contribute to Prdx1 release under ALI. In addition to

passive release of Prdx1 from damaged cells, secretion from active immune cells is another mechanism for most DAMPs [10]. Previous studies have reported that some stimuli including TGF-β1, LPS and TNF-α could induce the secretion of Prdx1 from macrophages *in vitro*. However, due to lack of signal peptides, the secretory mechanisms of Prdx1 remain elusive. Several studies found that the active secretion of Prdx1 is possibly mediated by a non-classical secretory pathway [26] or by an exosomal pathway [28]. Although the mechanisms are under active investigation, the process under which Prdx1 is released into the extracellular space requires further studies.

In conclusion, our study suggests that circulating Prdx1 aggravates acute liver injury as a novel DAMP, and that Prdx1 elicits hepatic inflammation at least in part via activating the NLRP3 inflammasome signaling pathway. In light of our discoveries for the importantly detrimental role of circulating Prdx1 in ALI, neutralization of circulating Prdx1 may be a potential treatment option, which merits further investigation.

Acknowledgements

This study was supported by grants from the National Natural Science Foundation of China (No. 81370547, 81873585, 81400642, 81673499 and 81470255) to H.Y. and Chinese Society of Nephrology (No. 1502009057) to H.Y.

Compliance with ethical standards

Conflict of interest

The authors declare that they have no conflict of interest.

References

1. McDonald B, Kubes P. Innate Immune Cell Trafficking and Function During Sterile Inflammation of the Liver. Gastroenterology 2016;151:1087-1095

2. Chung RT, Stravitz RT, Fontana RJ, et al. Pathogenesis of liver injury in acute liver failure. Gastroenterology 2012;143:e1-e7

3. Kim SY, Son M, Lee SE, et al. High-Mobility Group Box 1-Induced Complement Activation Causes Sterile Inflammation. Front Immunol 2018;9:705

4. Mihm S. Danger-Associated Molecular Patterns (DAMPs): Molecular Triggers for Sterile Inflammation in the Liver. Int J Mol Sci 2018;19

5. Tilg H, Moschen AR, Szabo G. Interleukin-1 and inflammasomes in alcoholic liver disease/acute alcoholic hepatitis and nonalcoholic fatty liver disease/nonalcoholic steatohepatitis. Hepatology 2016;64:955-965

6. Woolbright BL, Jaeschke H. The Impact of Sterile Inflammation in Acute Liver Injury. J Clin Transl Res 2017;3:170-188

7. Woolbright BL, Jaeschke H. Sterile inflammation in acute liver injury: myth or mystery? Expert Rev Gastroenterol Hepatol 2015;9:1027-1029

8. Williams CD, Antoine DJ, Shaw PJ, et al. Role of the Nalp3 inflammasome in acetaminophen-induced sterile inflammation and liver injury. Toxicol Appl Pharmacol 2011;252:289-297

9. Kubes P, Mehal WZ. Sterile inflammation in the liver. Gastroenterology 2012;143:1158-1172

10. Yang, Han Z, Oppenheim JJ. Alarmins and immunity. Immunol Rev 2017;280:41-56

11. Tang D, Kang R, Coyne CB, Zeh HJ, Lotze MT. PAMPs and DAMPs: signal 0s that spur autophagy and immunity. Immunol Rev 2012;249:158-175

12. Roh JS, Sohn DH. Damage-Associated Molecular Patterns in Inflammatory Diseases. Immune Netw 2018;18:e27

13. Dela CC, Kang MJ. Mitochondrial dysfunction and damage associated molecular patterns (DAMPs) in chronic inflammatory diseases. Mitochondrion 2018;41:37-44

14. Nakahira K, Hisata S, Choi AM. The Roles of Mitochondrial Damage-Associated Molecular Patterns in Diseases. Antioxid Redox Signal 2015;23:1329-1350

15. Szabo G, Petrasek J. Inflammasome activation and function in liver disease. Nat Rev

Gastroenterol Hepatol 2015;12:387-400

16. Ishii T, Yamada M, Sato H, et al. Cloning and characterization of a 23-kDa stress-induced mouse peritoneal macrophage protein. J Biol Chem 1993;268:18633-18636

17. Seo MS, Kang SW, Kim K, et al. Identification of a new type of mammalian peroxiredoxin that forms an intramolecular disulfide as a reaction intermediate. J Biol Chem 2000;275:20346-20354

18. Perkins A, Nelson KJ, Parsonage D, Poole LB, Karplus PA. Peroxiredoxins: guardians against oxidative stress and modulators of peroxide signaling. Trends Biochem Sci 2015;40:435-445

19. Yan Y, Sabharwal P, Rao M, Sockanathan S. The antioxidant enzyme Prdx1 controls neuronal differentiation by thiol-redox-dependent activation of GDE2. Cell 2009;138:1209-1221

20. Ding C, Fan X, Wu G. Peroxiredoxin 1 - an antioxidant enzyme in cancer. J Cell Mol Med 2017;21:193-202

21. O'Neill JS, Reddy AB. Circadian clocks in human red blood cells. Nature 2011;469:498-503

22. Mei W, Peng Z, Lu M, et al. Peroxiredoxin 1 inhibits the oxidative stress induced apoptosis in renal tubulointerstitial fibrosis. Nephrology (Carlton) 2015;20:832-842

23. Park MH, Jo M, Kim YR, Lee CK, Hong JT. Roles of peroxiredoxins in cancer, neurodegenerative diseases and inflammatory diseases. Pharmacol Ther 2016;163:1-23

24. Neumann CA, Krause DS, Carman CV, et al. Essential role for the peroxiredoxin Prdx1 in erythrocyte antioxidant defence and tumour suppression. Nature 2003;424:561-565

25. Chang JW, Lee SH, Jeong JY, et al. Peroxiredoxin-I is an autoimmunogenic tumor antigen in non-small cell lung cancer. Febs Lett 2005;579:2873-2877

26. Chang JW, Lee SH, Lu Y, Yoo YJ. Transforming growth factor-beta1 induces the non-classical secretion of peroxiredoxin-I in A549 cells. Biochem Biophys Res Commun 2006;345:118-123

27. Conde-Vancells J, Rodriguez-Suarez E, Embade N, et al. Characterization and comprehensive proteome profiling of exosomes secreted by hepatocytes. J Proteome Res 2008;7:5157-5166

28. Mullen L, Hanschmann EM, Lillig CH, Herzenberg LA, Ghezzi P. Cysteine Oxidation Targets Peroxiredoxins 1 and 2 for Exosomal Release through a Novel Mechanism of Redox-Dependent Secretion. Mol Med 2015;21:98-108

29. Riddell JR, Wang XY, Minderman H, Gollnick SO. Peroxiredoxin 1 stimulates secretion of proinflammatory cytokines by binding to TLR4. J Immunol 2010;184:1022-1030

30. Riddell JR, Bshara W, Moser MT, et al. Peroxiredoxin 1 controls prostate cancer growth

through Toll-like receptor 4-dependent regulation of tumor vasculature. Cancer Res 2011;71:1637-1646

31. Shichita T, Hasegawa E, Kimura A, et al. Peroxiredoxin family proteins are key initiators of post-ischemic inflammation in the brain. Nat Med 2012;18:911-917

32. Antoine DJ, Jenkins RE, Dear JW, et al. Molecular forms of HMGB1 and keratin-18 as mechanistic biomarkers for mode of cell death and prognosis during clinical acetaminophen hepatotoxicity. J Hepatol 2012;56:1070-1079

33. Lundback P, Lea JD, Sowinska A, et al. A novel high mobility group box 1 neutralizing chimeric antibody attenuates drug-induced liver injury and postinjury inflammation in mice. Hepatology 2016;64:1699-1710

34. Garcia-Martinez I, Santoro N, Chen Y, et al. Hepatocyte mitochondrial DNA drives nonalcoholic steatohepatitis by activation of TLR9. J Clin Invest 2016;126:859-864

35. He Y, Feng D, Li M, et al. Hepatic mitochondrial DNA/Toll-like receptor 9/MicroRNA-223 forms a negative feedback loop to limit neutrophil overactivation and acetaminophen hepatotoxicity in mice. Hepatology 2017;66:220-234

36. Ambade A, Catalano D, Lim A, Mandrekar P. Inhibition of heat shock protein (molecular weight 90 kDa) attenuates proinflammatory cytokines and prevents lipopolysaccharide-induced liver injury in mice. Hepatology 2012;55:1585-1595

37. Garcia-Bonilla L, Iadecola C. Peroxiredoxin sets the brain on fire after stroke. Nat Med 2012;18:858-859

38. Yanagisawa R, Warabi E, Inoue K, et al. Peroxiredoxin I null mice exhibits reduced acute lung inflammation following ozone exposure. J Biochem 2012;152:595-601

39. Liu D, Mao P, Huang Y, et al. Proteomic analysis of lung tissue in a rat acute lung injury model: identification of PRDX1 as a promoter of inflammation. Mediators Inflamm 2014;2014:469358

40. Benesic A, Leitl A, Gerbes AL. Monocyte-derived hepatocyte-like cells for causality assessment of idiosyncratic drug-induced liver injury. Gut 2016;65:1555-1563

41. Peng Y, Yang H, Wang N, et al. Fluorofenidone attenuates hepatic fibrosis by suppressing the proliferation and activation of hepatic stellate cells. Am J Physiol Gastrointest Liver Physiol 2014;306:G253-G263

42. Huang L, Zhang F, Tang Y, et al. Fluorofenidone attenuates inflammation by inhibiting the

NF-small ka, CyrillicB pathway. Am J Med Sci 2014;348:75-80

43. Lu M, Yang W, Peng Z, et al. Fluorofenidone inhibits macrophage IL-1beta production by suppressing inflammasome activity. Int Immunopharmacol 2015;27:148-153

44. Zhang J, Zheng L, Yuan X, et al. Mefunidone ameliorates renal inflammation and tubulointerstitial fibrosis via suppression of IKKbeta phosphorylation. Int J Biochem Cell Biol 2016;80:109-118

45. Richard S, Lapierre V, Girerd N, et al. Diagnostic performance of peroxiredoxin 1 to determine time-of-onset of acute cerebral infarction. Sci Rep 2016;6:38300

46. Zhao LX, Du JR, Zhou HJ, et al. Differences in Proinflammatory Property of Six Subtypes of Peroxiredoxins and Anti-Inflammatory Effect of Ligustilide in Macrophages. Plos One 2016;11:e164586

47. Larson AM, Polson J, Fontana RJ, et al. Acetaminophen-induced acute liver failure: results of a United States multicenter, prospective study. Hepatology 2005;42:1364-1372

48. Wu KC, Ho YL, Kuo YH, et al. Hepatoprotective Effect of Ugonin M, A Helminthostachyszeylanica Constituent, on Acetaminophen-Induced Acute Liver Injury in Mice. Molecules 2018;23

49. Cho YE, Seo W, Kim DK, et al. Exogenous exosomes from mice with acetaminophen-induced liver injury promote toxicity in the recipient hepatocytes and mice. Sci Rep 2018;8:16070

50. Bruckner JV, MacKenzie WF, Muralidhara S, et al. Oral toxicity of carbon tetrachloride: acute, subacute, and subchronic studies in rats. Fundam Appl Toxicol 1986;6:16-34

51. Martinez AK, Maroni L, Marzioni M, et al. Mouse models of liver fibrosis mimic human liver fibrosis of different etiologies. Curr Pathobiol Rep 2014;2:143-153

52. Kopec AK, Joshi N, Luyendyk JP. Role of hemostatic factors in hepatic injury and disease: animal models de-liver. J Thromb Haemost 2016;14:1337-1349

53. Liu CH, Kuo SW, Hsu LM, et al. Peroxiredoxin 1 induces inflammatory cytokine response and predicts outcome of cardiogenic shock patients necessitating extracorporeal membrane oxygenation: an observational cohort study and translational approach. J Transl Med 2016;14:114

54. Shichita T, Ito M, Morita R, et al. MAFB prevents excess inflammation after ischemic stroke by accelerating clearance of damage signals through MSR1. Nat Med 2017;23:723-732

55. Katarey D, Verma S. Drug-induced liver injury. Clin Med (Lond) 2016;16:s104-s109

56. Navarro VJ, Khan I, Bjornsson E, et al. Liver injury from herbal and dietary supplements. Hepatology 2017;65:363-373

57. Stickel F, Shouval D. Hepatotoxicity of herbal and dietary supplements: an update. Arch Toxicol 2015;89:851-865

58. Radyuk SN, Orr WC. The Multifaceted Impact of Peroxiredoxins on Aging and Disease. Antioxid Redox Signal 2018;29:1293-1311

59. Spahis S, Delvin E, Borys JM, Levy E. Oxidative Stress as a Critical Factor in Nonalcoholic Fatty Liver Disease Pathogenesis. Antioxid Redox Signal 2017;26:519-541

60. Forman HJ, Augusto O, Brigelius-Flohe R, et al. Even free radicals should follow some rules: a guide to free radical research terminology and methodology. Free Radic Biol Med 2015;78:233-235

61. Riddell JR, Maier P, Sass SN, et al. Peroxiredoxin 1 stimulates endothelial cell expression of VEGF via TLR4 dependent activation of HIF-1alpha. Plos One 2012;7:e50394

62. Dos ACA. F4/80 as a Major Macrophage Marker: The Case of the Peritoneum and Spleen. Results Probl Cell Differ 2017;62:161-179

63. Tacke F, Zimmermann HW. Macrophage heterogeneity in liver injury and fibrosis. J Hepatol 2014;60:1090-1096

64. Sun YY, Li XF, Meng XM, et al. Macrophage Phenotype in Liver Injury and Repair. Scand J Immunol 2017;85:166-174

65. Tacke F. Targeting hepatic macrophages to treat liver diseases. J Hepatol 2017;66:1300-1312

66. Possamai LA, Thursz MR, Wendon JA, Antoniades CG. Modulation of monocyte/macrophage function: a therapeutic strategy in the treatment of acute liver failure. J Hepatol 2014;61:439-445

67. Taniguchi K, Karin M. NF-kappaB, inflammation, immunity and cancer: coming of age. Nat Rev Immunol 2018;18:309-324

68. Zhang Q, Lenardo MJ, Baltimore D. 30 Years of NF-kappaB: A Blossoming of Relevance to Human Pathobiology. Cell 2017;168:37-57

69. Goffi F, Boroni F, Benarese M, et al. The inhibitor of I kappa B alpha phosphorylation BAY 11-7082 prevents NMDA neurotoxicity in mouse hippocampal slices. Neurosci Lett 2005;377:147-151

70. Mori N, Yamada Y, Ikeda S, et al. Bay 11-7082 inhibits transcription factor NF-kappaB and induces apoptosis of HTLV-I-infected T-cell lines and primary adult T-cell leukemia cells. Blood

2002;100:1828-1834

71. Feldman N, Rotter-Maskowitz A, Okun E. DAMPs as mediators of sterile inflammation in aging-related pathologies. Ageing Res Rev 2015;24:29-39

72. Youm YH, Grant RW, McCabe LR, et al. Canonical Nlrp3 inflammasome links systemic low-grade inflammation to functional decline in aging. Cell Metab 2013;18:519-532

73. He Y, Hara H, Nunez G. Mechanism and Regulation of NLRP3 Inflammasome Activation. Trends Biochem Sci 2016;41:1012-1021

74. Man SM, Kanneganti TD. Regulation of inflammasome activation. Immunol Rev 2015;265:6-21

75. Koch DG, Speiser JL, Durkalski V, et al. The Natural History of Severe Acute Liver Injury. Am J Gastroenterol 2017;112:1389-1396

76. Best J, Dolle L, Manka P, et al. Role of liver progenitors in acute liver injury. Front Physiol 2013;4:258

77. Bernal W, Auzinger G, Dhawan A, Wendon J. Acute liver failure. Lancet 2010;376:190-201

78. Kim SU, Park YH, Min JS, et al. Peroxiredoxin I is a ROS/p38 MAPK-dependent inducible antioxidant that regulates NF-kappaB-mediated iNOS induction and microglial activation. J Neuroimmunol 2013;259:26-36

79. Bast A, Fischer K, Erttmann SF, Walther R. Induction of peroxiredoxin I gene expression by LPS involves the Src/PI3K/JNK signalling pathway. Biochim Biophys Acta 2010;1799:402-410

80. Dayon L, Turck N, Garci-Berrocoso T, et al. Brain extracellular fluid protein changes in acute stroke patients. J Proteome Res 2011;10:1043-1051

81. Lin X, Wei F, Major P, et al. Microvesicles Contribute to the Bystander Effect of DNA Damage. Int J Mol Sci 2017;18

Figure Legends

Figure1: A significant elevation of circulating Prdx1 in mice with ALI induced by APAP or CCl_4. A-D: Wild-type (WT) mice were injected with saline or APAP (500mg/Kg, i.p.) and then sacrificed on 12 or 24 hours, n=6/group. 0h=saline control group, 12h=12-hours group, 24h=24-hours group. **A**: Histological images of liver sections stained with H&E, scale bar: 100μm (200x). **B-C**: Serum ALT and AST levels in mice. **D**: Circulating Prdx1 level was measured by ELISA. **E-H**: WT mice were injected with olive oil or CCl_4 (0.5ml/Kg, i.p.) and then sacrificed on days 2, 4 and 7, n=5/group. 0=olive oil control group, 2=2-days group, 4=4-days group, 7=7-days group. **E**: Histological images of liver sections stained with H&E, scale bar: 100μm (200x). **F-G**: Serum ALT and AST levels in mice. **H**: Circulating Prdx1 level was measured by ELISA. Data are expressed as the mean ± SD; ns: no significance. *: vs. control group, $^{\#}$: vs. 12-hours group. ns: no significance, $^{*}P<0.05$, $^{**}P<0.01$, $^{***}P<0.001$; $^{\#}P<0.05$, $^{\#\#}P<0.01$.

Figure2: Prdx1 deficiency plays a protective role in ALI induced by APAP. In APAP-induced ALI model, WT and Prdx1-knockout (*Prdx1*$^{-/-}$) mice were injected with saline or APAP (500mg/Kg, i.p.) for one time and sacrificed at 12 or 24 hours, n=6/group. 0h=saline control group, 12h=12-hours group, 24h=24-hours group. **A:** Histological images of liver sections stained with H&E, scale bar: 100μm (200x). **B-E**: Serum ALT, AST, TBIL and DBIL levels in mice. Data are expressed as the mean ± SD; ns: no significance, *: vs. control group, $^{\$}$: vs. 12-hours group, $^{\#}$: vs. WT group. ns: no significance, $^{*}P<0.05$, $^{**}P<0.01$, $^{***}P<0.001$; $^{\$}P<0.05$; $^{\#}P<0.05$, $^{\#\#}P<0.01$.

Figure3: Prdx1 deficiency plays a protective role in ALI induced by CCl_4. WT and *Prdx1*$^{-/-}$ mice were injected with olive oil or CCl_4 (0.5ml/Kg, i.p.) for one time and sacrificed after 2 days, n=5/group. **A**: Histological images of liver sections stained with H&E, scale bar: 100μm (200x). **B-E**: Serum ALT, AST, TBIL and DBIL levels in mice. Data are expressed as the mean ± SD; ns: no significance, *: vs. control

group, $^{\#}$: vs. WT group. ns: no significance, $^{*}P<0.05$, $^{**}P<0.01$, $^{***}P<0.001$; $^{\#}P<0.05$, $^{\#\#}P<0.01$.

Figure4: rPrdx1 aggravates liver injury in APAP-induced ALI. After APAP treatment (500mg/Kg, i.p.), *Prdx1*$^{-/-}$ mice were intravenously injected with PBS or rPrdx1 (10μg/Kg) for 24 hours, n=6/group. **A:** Histological images of liver sections stained with H&E, scale bar: 100μm (200x). **B-C**: Serum ALT and AST levels in mice. Data are expressed as the mean ± SD, ns: no significance, *: vs. PBS control group, $^{\#}$: vs. APAP group. $^{*}P<0.05$, $^{**}P<0.01$, $^{***}P<0.01$; $^{\#}P<0.05$, $^{\#\#}P<0.05$.

Figure5: APAP induces the release of Prdx1 from hepatocytes and the decreased expression of hepatic Prdx1 in ALI mouse model. A: Primary mouse hepatocytes were exposed to different doses of APAP (5mM, 10mM and 15mM) for 24 hours (n=4 independent experiments) and then the level of released Prdx1 in culture medium was measured by ELISA; *: vs. control group, $^{\#}$: vs. 5mM APAP group. **B**: Primary mouse hepatocytes were exposed to 5mM APAP for 6, 12, 24 hours (n=3 independent experiments) and then the level of released Prdx1 in culture medium was measured by ELISA; *: vs. control group, $^{\#}$: vs. 6 hours group. **C-D**: WT mice were injected with saline or APAP (500mg/Kg, i.p.) and then sacrificed on 12 or 24 hours, n=6/group. 0h=saline control group, 12h=12-hours group, 24h=24-hours group. **C**: Prdx1 protein level in liver tissue was measured by western blotting; *: vs. saline control group, $^{\#}$: vs. APAP 12 hours group. **D**: Immunohistochemical staining for Prdx1 in liver, scale bar: 50μm (400x). $^{*}P<0.05$, $^{**}P<0.01$, $^{***}P<0.01$; $^{\#}P<0.05$, $^{\#\#}P<0.05$, $^{\#\#\#}P<0.05$.

Figure6: Association of circulating Prdx1 with inflammation in ALI. A-D: In APAP-induced ALI model, WT and *Prdx1*$^{-/-}$ mice were injected with saline or APAP (500mg/Kg, i.p.) for one time and sacrificed at 12 or 24 hours, n=6/group. 0h=saline control group, 12h=12-hours group, 24h=24-hours group. **A**: Quantitation of macrophages infiltration indicated by F4/80 staining; *: vs. saline control group, $^{\$}$: vs.

12-hours group, $^{\#}$: vs. WT control group. **B-D**: mRNA levels of IL-1β, IL-6, and TNF-α in liver tissue were measured by RT-PCR; *: vs. WT control group. **E-H**: WT and *Prdx1*$^{-/-}$ mice were injected with olive oil or CCl_4 (0.5ml/Kg, i.p.) for one time and sacrificed after 2 days, n=5/group. **E**: Quantitation of macrophages infiltration indicated by F4/80 staining; *: vs. saline control group, $^{\#}$: vs. WT control group. **F-H**: mRNA levels of IL-1β, IL-6, and TNF-α in liver tissue were measured by RT-PCR; *: vs. WT control group. **I-J**: After APAP treatment (500mg/Kg, i.p.), *Prdx1*$^{-/-}$ mice were intravenously injected with PBS or rPrdx1 (10μg/Kg) for 24 hours, n=6/group. *: vs. PBS control group, $^{\#}$: vs. APAP + PBS group. **I**: Quantitation of macrophages infiltration indicated by F4/80 staining. **J-H**: mRNA levels of IL-1β, IL-6, and TNF-α in liver tissue were measured by RT-PCR. $^{*}P<0.05$, $^{**}P<0.01$, $^{***}P<0.01$; $^{\#}P<0.05$, $^{\#\#}P<0.05$, $^{\#\#\#}P<0.05$; $^{\$}P<0.05$, $^{\$\$}P<0.05$.

Figure7: Prdx1 induces inflammatory cytokines production in primary peritoneal macrophages through the NF-κB and NLRP3 inflammsome signaling pathways. A: Primary peritoneal macrophages from WT mice were stimulated with different doses of rPrdx1 (25nM, 50nM) for 24 hours and after that the expression of pro-IL-1β was detected by western-blotting; *: vs. control group, $^{\#}$: vs. 25nM rPrdx1 group. **B-F:** Primary peritoneal macrophages from WT mice were stimulated with rPrdx1 (25nM) for different times; *: vs. control group, $^{\#}$: vs. 24hours rPrdx1 group. **B-C**: Levels of IL-6 and TNF-α in the cellular supernatant were measured by ELISA. **D:** The expression of pro-IL-1β was detected by western blotting. **E**: Level of mature IL-1β in the cellular supernatant was measured by ELISA. **F:** The expression of pro-IL-1β, pro-caspase-1, NLRP3, mature IL-1β and cleaved caspase-1 were detected by western blotting. The inflammatory cytokines released by macrophages were stimulated by rPrdx1, with or without pretreatment of BAY (BAY 11-7082, 50μM for 1hours), PMB (10μg/ml for 1hours), heat (95°C for 10min) and MCC950 (10μM for 1hour). All experiments were repeated four times. Abbreviations: sn: cell supernatant; ns: no significance. Data are expressed as the mean ± SD, $^{*}P<0.05$, $^{**}P<0.01$, $^{***}P<0.01$; $^{\#}P<0.05$, $^{\#\#}P<0.01$, $^{\#\#\#}P<0.001$.

Figure8: Circulating Prdx1 contributes to poor outcomes in ALI. A: To observe survival rate, WT and *Prdx1*$^{-/-}$ mice were injected with APAP (750mg/Kg, i.p.) for one time, n=14/group. **B**: Survival rate in *Prdx1*$^{-/-}$ mice intravenously injected with PBS or rPrdx1 (10μg/Kg≈200ng per mouse or 20μg/Kg≈400ng per mouse) after APAP treatment (750mg/Kg, i.p.), n=14/group; *: vs. APAP + PBS control group. $^{*}P<0.05$.

Figure9: Elevation of circulating Prdx1 in patients with ALI. A: Circulating Prdx1 levels in normal subjects (n=15) and patients with ALI (n=15), patients with liver cirrhosis (n=15) were measured by ELISA; *: vs. normal subjects, $^{\#}$: vs. ALI group. **B:** The linear correlations between Prdx1 and ALT in patients with ALI. **C:** The linear correlations between Prdx1 and AST in patients with ALI. **D:** The linear correlations between Prdx1 and TBIL patients with ALI. The linear correlation was analyzed by Pearson's correlation coefficient. Abbreviations: ALI: acute liver injury; ALT: alanine aminotransferase; AST: aspartate aminotransferase; TBIL: total bilirubin; Data are expressed as the mean ± SD; ns: no significance, $^{*}P<0.05$, $^{***}P<0.001$, $^{\#}P<0.05$.

Table1. Characteristics of the human subjects

Variable	Normal(n=15)	ALI(n=15)	Liver cirrhosis(n=15)	P-value
Gender, n (%)				
Male	8(53.3)	12(80)	13(86.7)	-
Female	7(46.7)	3(20)	2(13.3)	-
Age (years)	49.73±8.61	42.40±10.16	54.60±11.18	0.036^{*}/0.192
Blood Pressure				
SBP (mmHg)	126.20±13.02	116.60±12.56	114.93±12.07	0.038^{*}/$0.021^{\#}$
DBP (mmHg)	79.53±12.36	74.67±6.72	72.07±10.88	0.223/0.090
LFT				
TP(g/L)	64.05±3.77	66.77±7.22	58.09±6.90	0.360/$0.007^{\#\#}$
ALB(g/L)	39.99±2.45	35.51±4.56	29.37±4.10	0.003^{**}/$<0.001^{\#\#\#}$
TBIL (μmol/L)	12.89±5.82	218.61±193.31	23.70±20.58	0.001^{**}/0.06
DBIL (μmol/L)	5.36±2.27	105.57±87.86	10.81±6.65	0.001^{**}/$0.006^{\#\#}$
TBA (μmol/ L)	3.27±2.02	107.77±77.35	29.66±32.17	$<0.001^{***}$/$0.004^{\#\#}$
ALT (U/L)	20.27±13.10	611.74±572.81	23.29±9.88	0.001^{**}/0.483
AST (U/L)	22.67±7.32	350.15±348.98	36.70±11.92	0.002^{**}/$<0.001^{\#\#\#}$
ALP (U/L)	124.28±16.32	210.17±74.00	215.03±231.81	0.003^{**}/0.286
GGT (U/L)	20.63±18.39	126.60±72.36	98.81±162.23	$<0.001^{***}$/0.193
CBC				
WBC (10^9/L)	6.63±2.16	7.11±2.53	3.38±0.86	0.474/$<0.001^{\#\#\#}$
RBC (10^12/L)	4.40±0.42	4.27±0.72	3.17±0.64	0.449/$<0.001^{\#\#\#}$
HB(g/L)	133.60±11.42	130.60±20.51	88.67±23.65	0.527/$<0.001^{\#\#\#}$
PLT (10^9/L)	177.20±38.30	195.27±72.33	63.87±61.54	0.258/$<0.001^{\#\#\#}$
Coagulation test				
PT(second)	12.97±0.84	16.51±6.69	18.52±4.26	0.087/$<0.001^{\#\#\#}$
PTA (%)	105.39±9.53	81.31±26.85	60.88±1.48	0.015^{*}/$<0.001^{\#\#\#}$
INR	1.01±0.07	1.31±0.57	1.48±2.50	0.089/$<0.001^{\#\#\#}$
AFP(ng/ml)	1.05±1.58	248.25±307.75	2.50±2.14	0.021^{*}/0.091

Abbreviations: ALI: acute liver injury; SBP: systolic blood pressure; DBP: diastolic blood pressure; LFT: liver function test; TP: total protein; ALB: albumin; TBIL: total bilirubin; DBIL: direct bilirubin; TBA: total bile acid; ALT: alanine aminotransferase; AST: aspartate aminotransferase; ALP: alkaline phosphatase; GGT: gamma-glutamyltransferase; CBC: complete blood count; WBC: white blood cell; RBC: red blood cell; HB: hemoglobin; PLT: platelet; PT: prothrombin time; PTA: prothrombin time activity percentage; INR: international normalized ratio; AFP: alpha fetoprotein. Data are presented as means±SD. *: ALI vs. normal subjects, $^{\#}$: cirrhosis vs. normal subjects; $^{*}P<0.05$, $^{**}P<0.01$, $^{***}P<0.001$, $^{\#}P<0.05$, $^{\#\#}P<0.01$, $^{\#\#\#}P<0.001$;

Table2. Details of patients with ALI classified by etiology.

Variable	Etiology		*P*-value
	Hepatitis B virus	Drug	
N(%)	9(60)	6(40)	-
Prdx1(ng/ml)	34.78±16.33	33.14±16.45	0.852
ALT(U/L)	822.94±688.01	294.93±63.32	0.078
AST(U/L)	458.20±414.27	188.08±117.81	0.148
TBIL(μmol/L)	317.04±185.58	70.95±76.94**	0.009
DBIL(μmol/L)	151.99±79.49	34.95±42.50**	0.006
ALP(U/L)	223.22±81.26	186.68±59.31	0.397
GGT(U/L)	127.13±60.91	125.64±97.96	0.972

Abbreviations: ALI: acute liver injury; ALT: alanine aminotransferase; AST: aspartate aminotransferase; TBIL: total bilirubin; DBIL: direct bilirubin; ALP: alkaline phosphatase; GGT: gamma-glutamyltransferase. Data are presented as means±SD. *: Hepatitis B virus group vs. drug group: *P<0.05, **P <0.01.

Figure 1

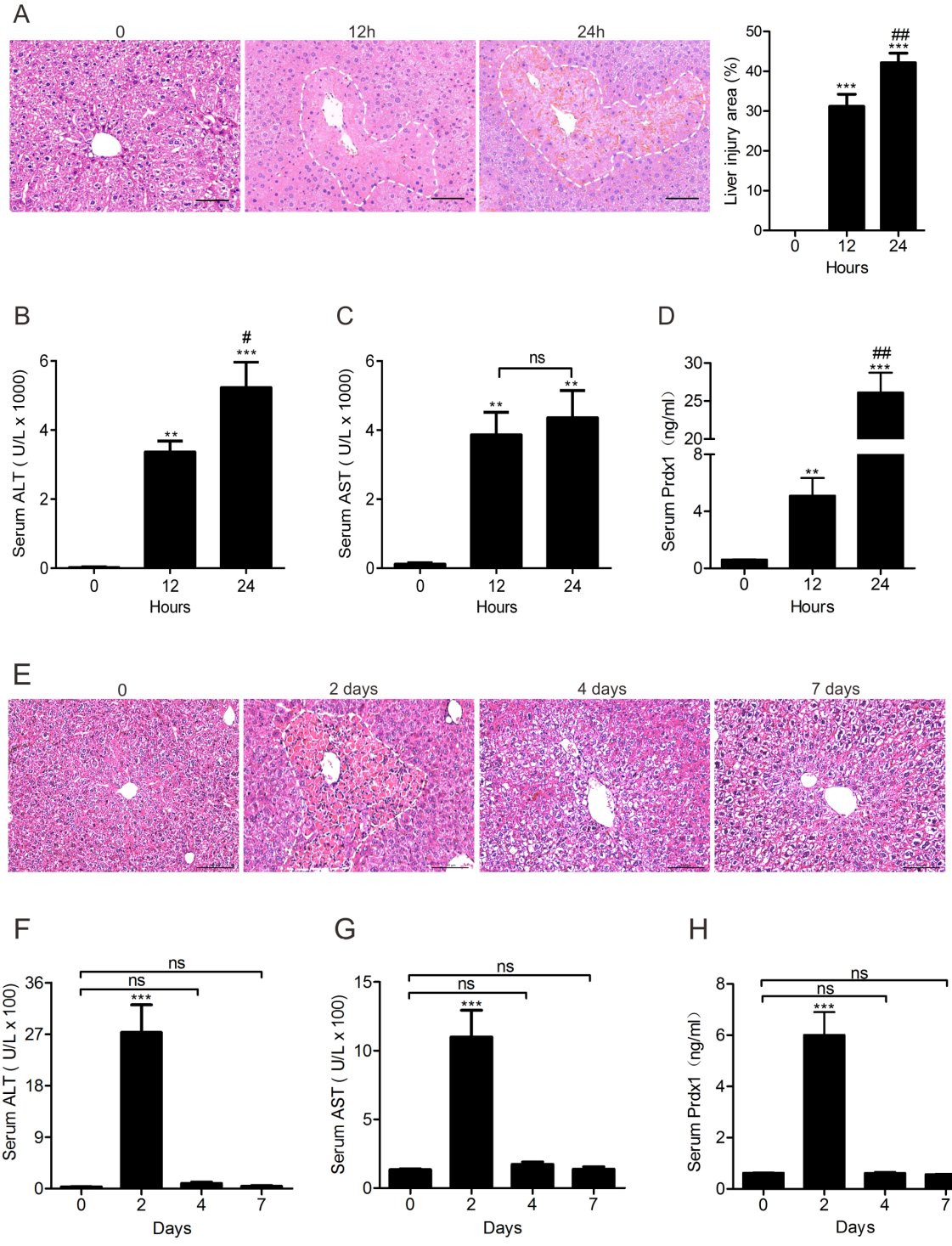
A
0
12h
24h
Liver injury area (%)
Hours
B
Serum ALT (U/L x 1000)
Hours
C
Serum AST (U/L x 1000)
ns
Hours
D
Serum Prdx1 (ng/ml)
Hours
E
0
2 days
4 days
7 days
F
Serum ALT (U/L x 100)
ns
Days
G
Serum AST (U/L x 100)
ns
Days
H
Serum Prdx1 (ng/ml)
ns
Days

Figure 2

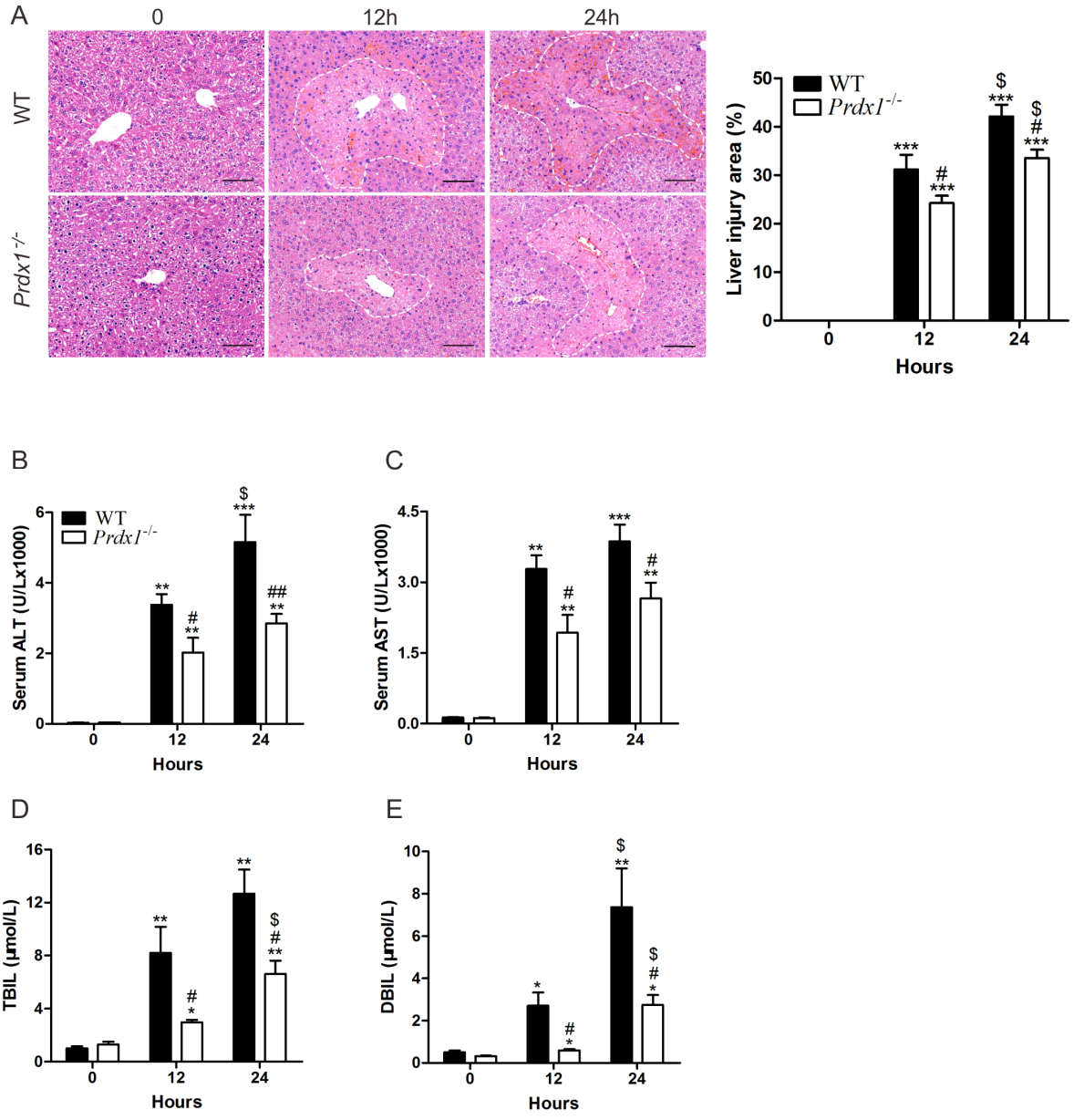
A
0
12h
24h
WT
Prdx1-/-
Liver injury area (%)
WT
Prdx1-/-
Hours
B
Serum ALT (U/Lx1000)
C
Serum AST (U/Lx1000)
D
TBIL (μmol/L)
E
DBIL (μmol/L)

Figure 3

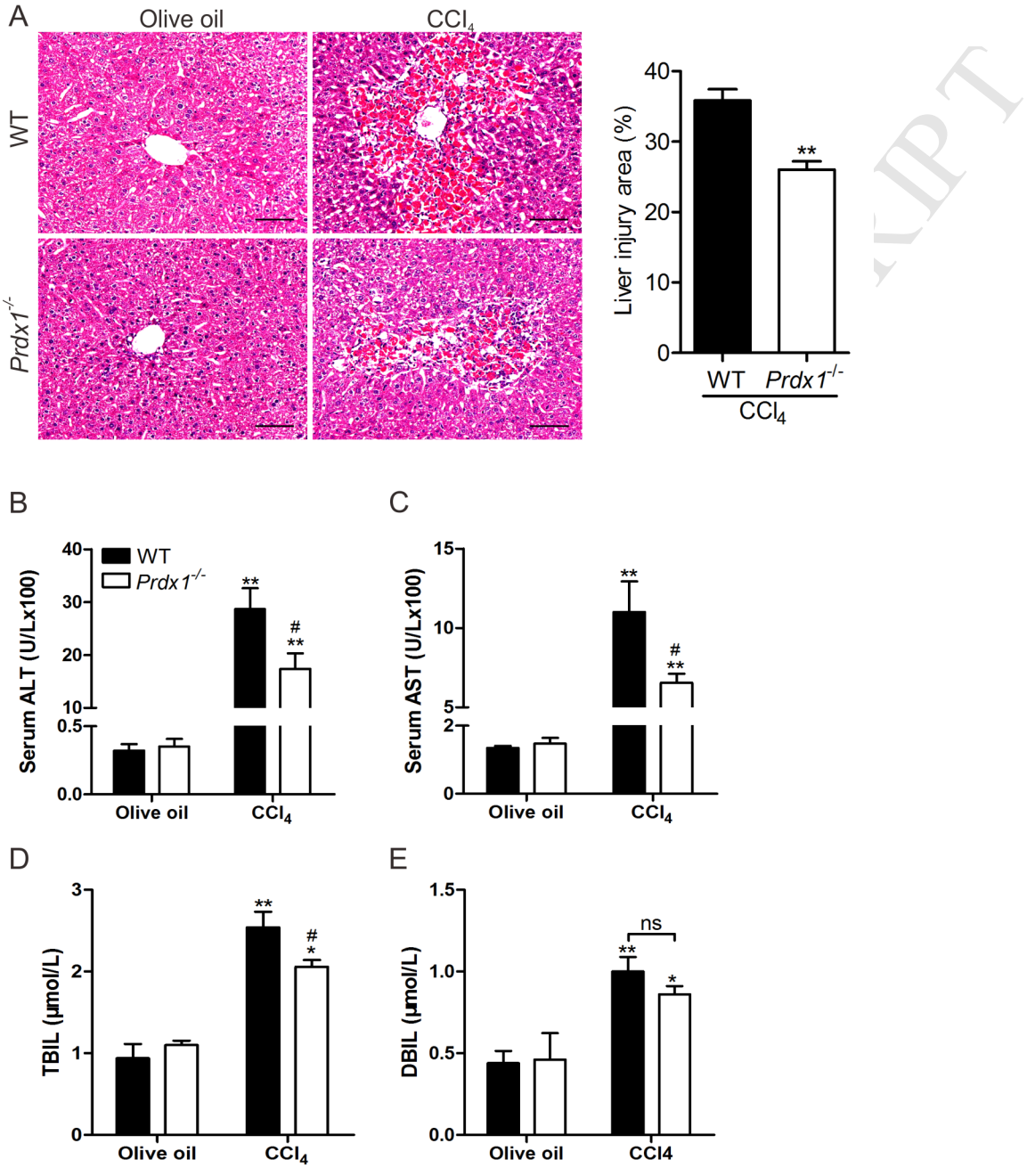
A
Olive oil
CCl4
WT
Prdx1-/-
Liver injury area (%)
40
30
20
10
0
**
WT
Prdx1-/-
CCl4
B
Serum ALT (U/Lx100)
WT
Prdx1-/-
40
30
20
10
0.5
0.0
**
#
**
Olive oil
CCl4
C
Serum AST (U/Lx100)
15
10
5
2
0
**
#
**
Olive oil
CCl4
D
TBIL (μmol/L)
3
2
1
0
**
#
*
Olive oil
CCl4
E
DBIL (μmol/L)
1.5
1.0
0.5
0.0
ns
**
*
Olive oil
CCl4

Figure 4

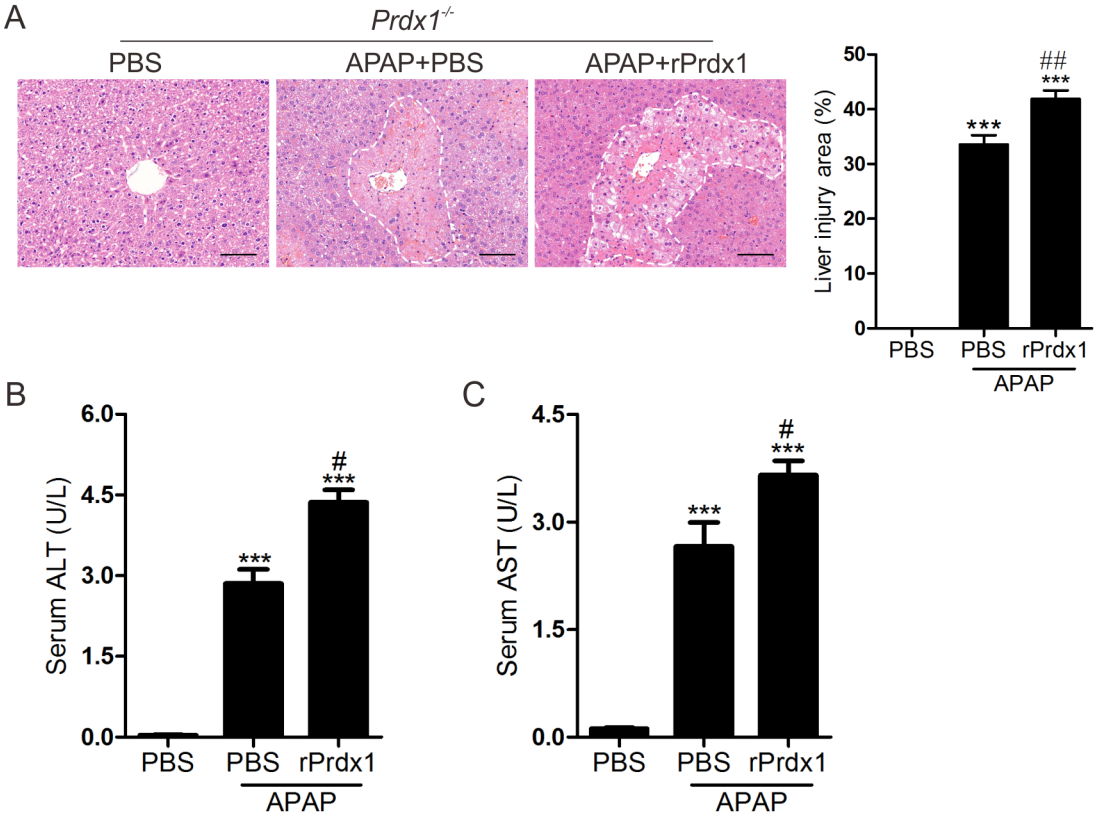

Figure 5

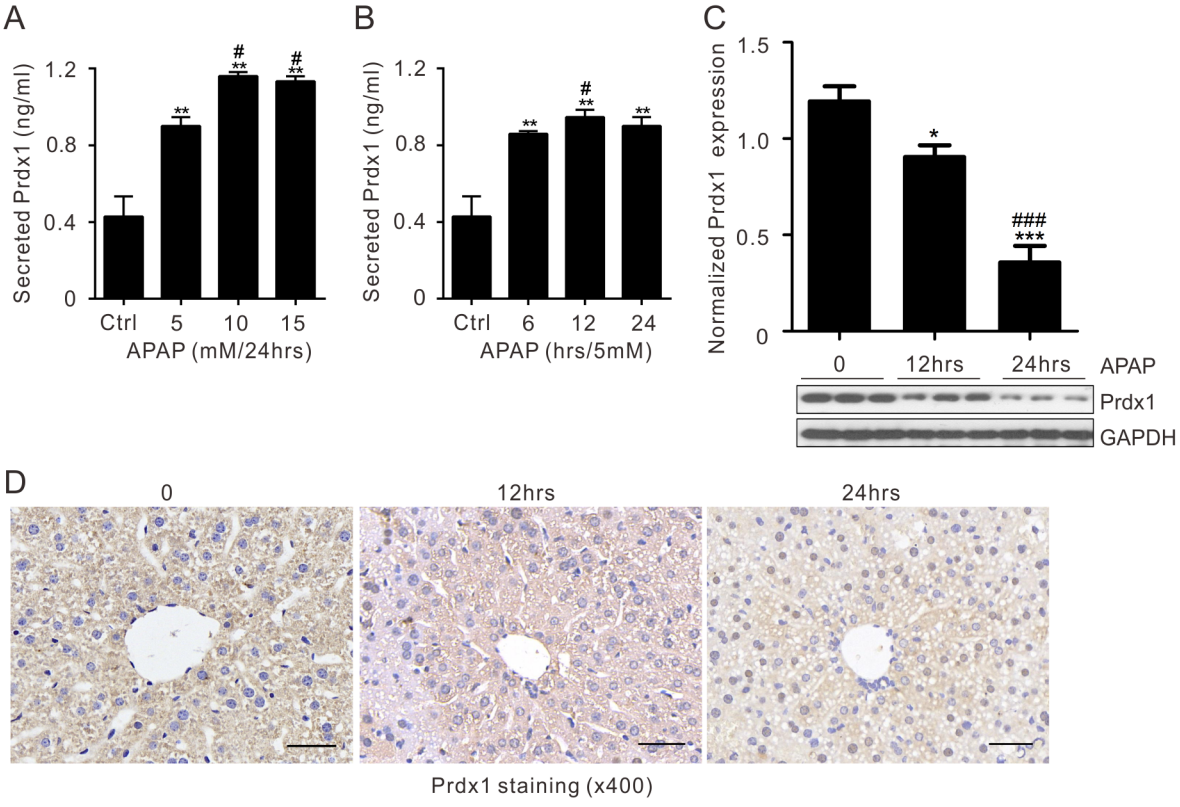

Figure 6

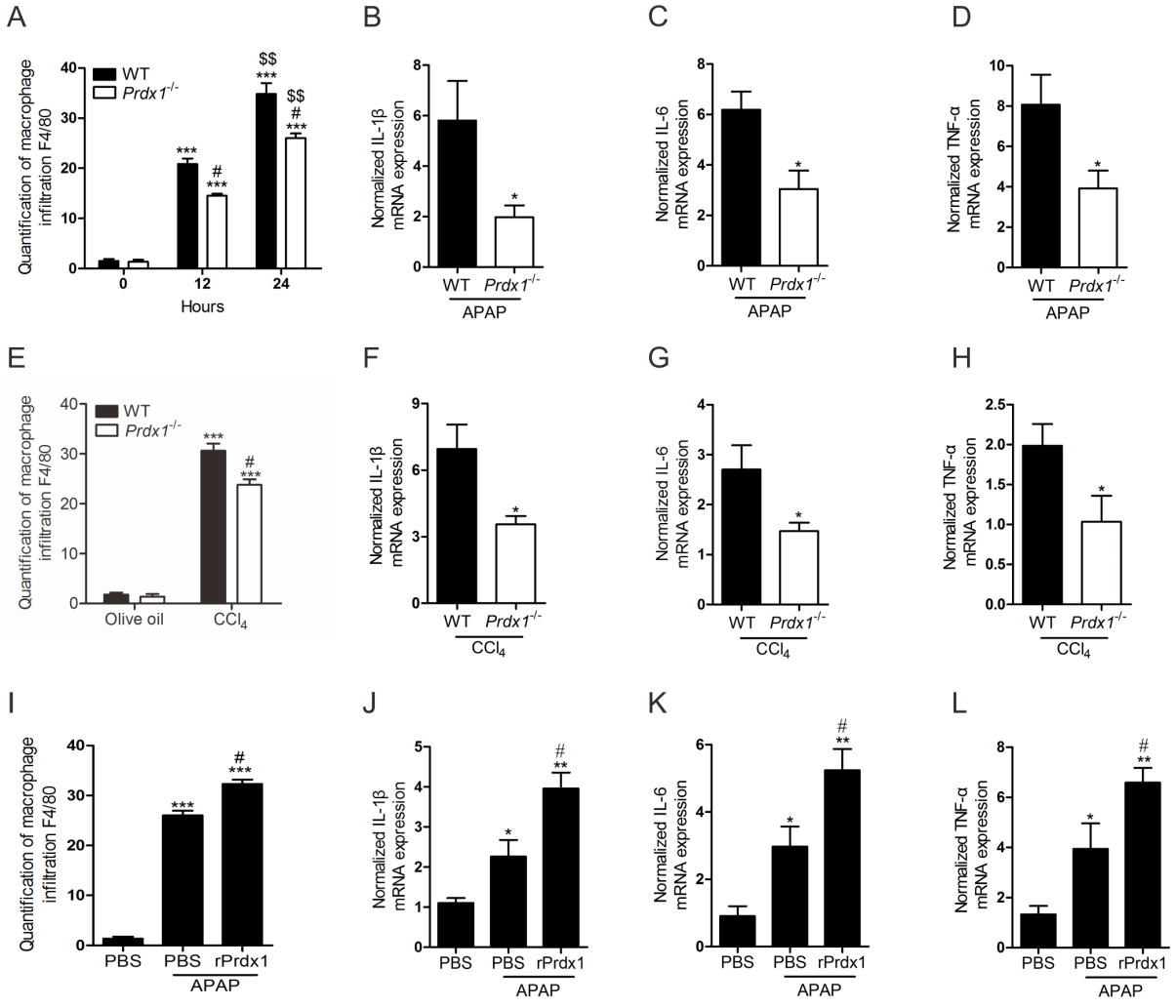

Figure 7

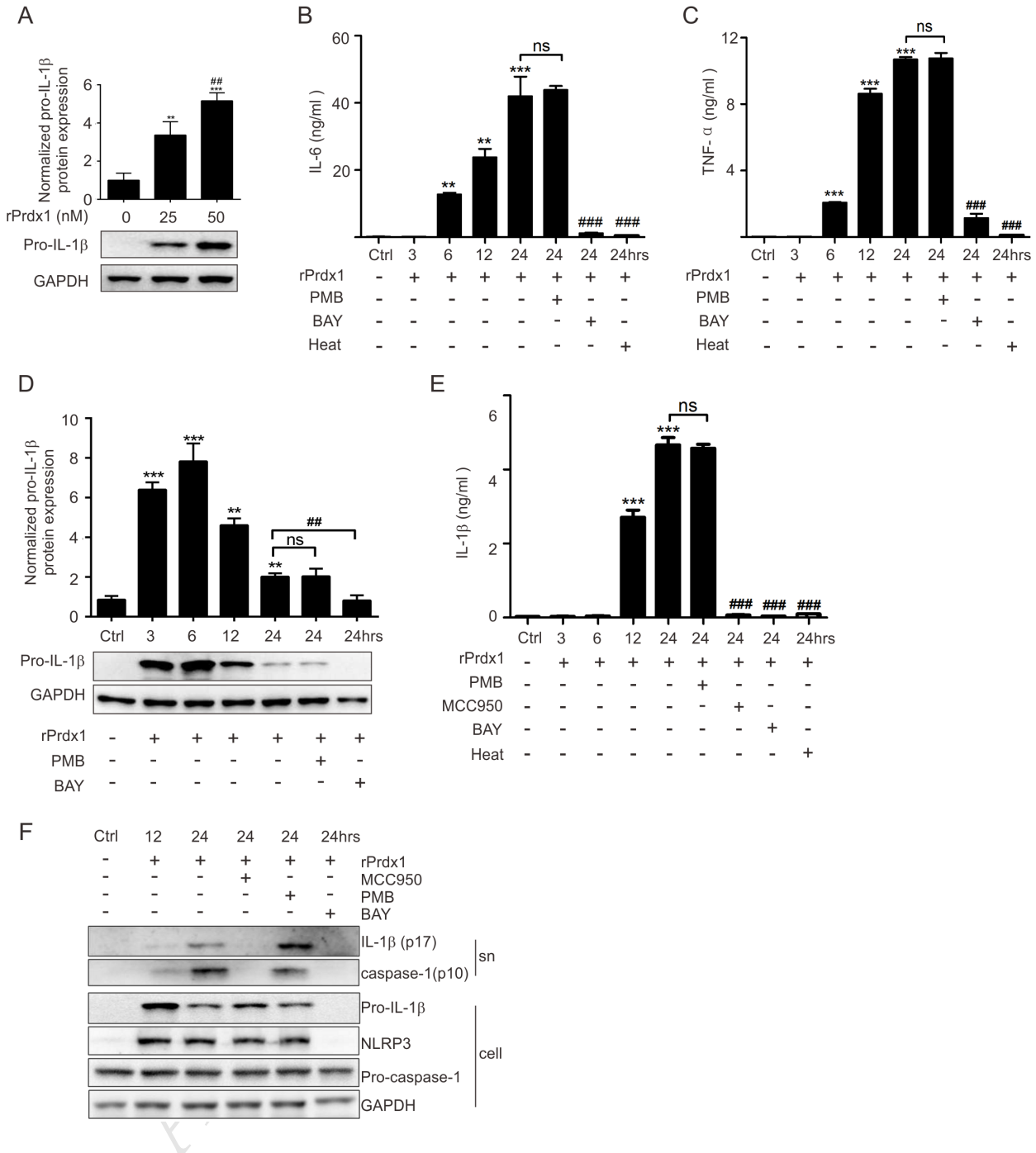
A
Normalized pro-IL-1β protein expression
rPrdx1 (nM)
0
25
50
Pro-IL-1β
GAPDH
B
IL-6 (ng/ml)
Ctrl
3
6
12
24
24
24
24hrs
rPrdx1
PMB
BAY
Heat
C
TNF- α (ng/ml)
D
Normalized pro-IL-1β protein expression
E
IL-1β (ng/ml)
MCC950
F
IL-1β (p17)
caspase-1(p10)
sn
Pro-IL-1β
NLRP3
Pro-caspase-1
GAPDH
cell

Figure 8

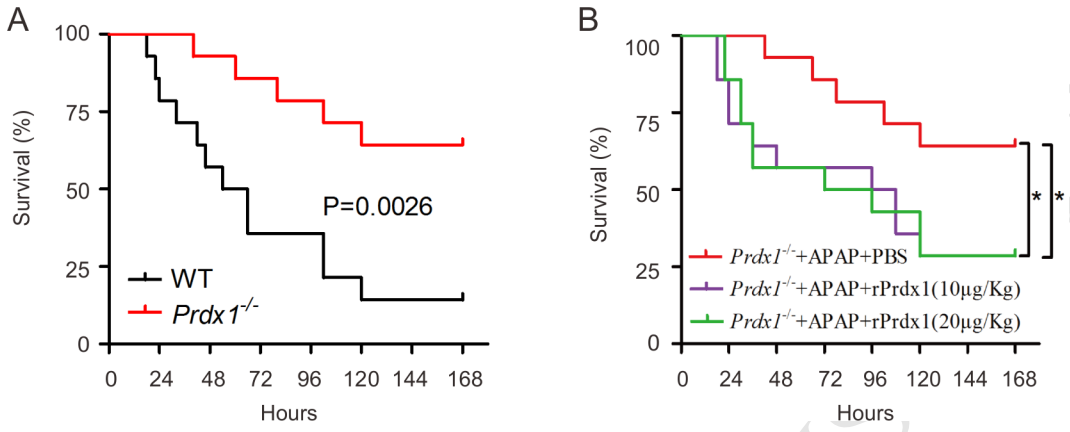

Figure 9

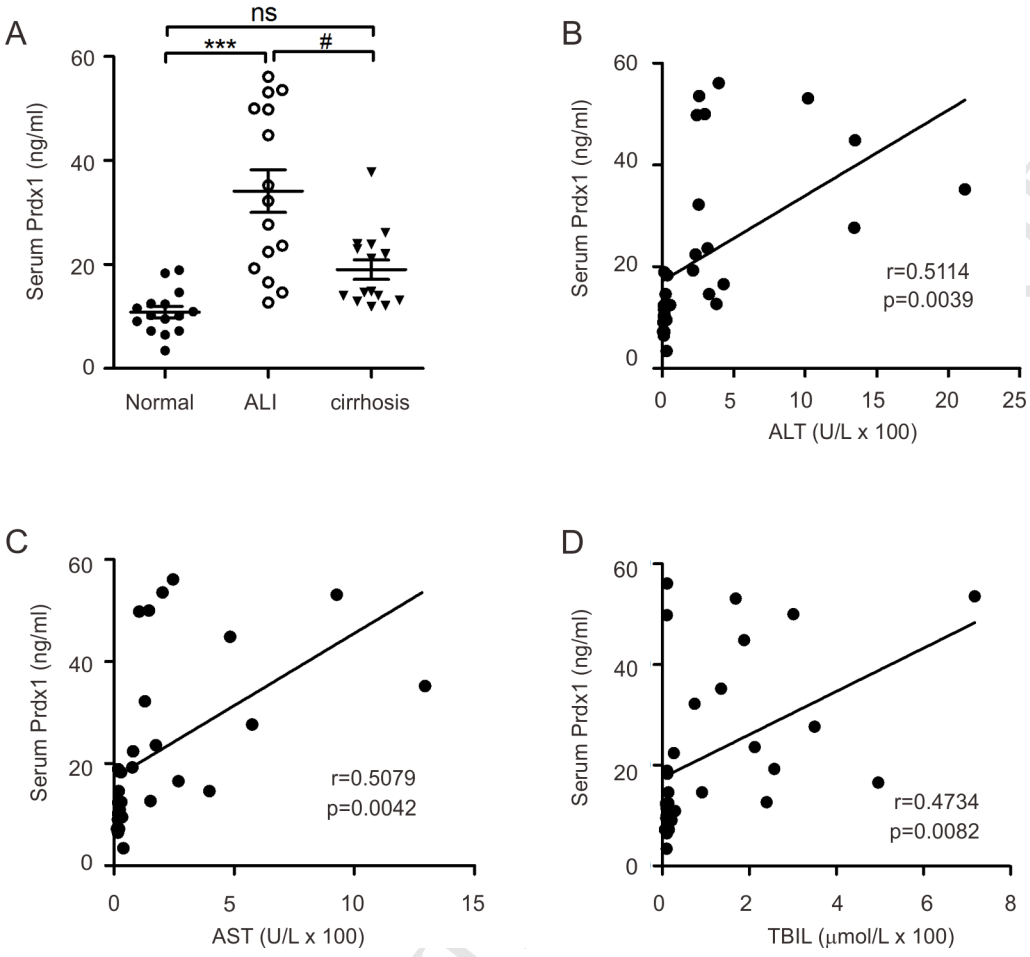

Highlights

- Increases in serum Prdx1 in patients and mice with acute liver injury (ALI).
- *Prdx1*$^{-/-}$ mice are protected from drug-induced ALI and ALI-associated inflammation.
- Intravenous injection of recombinant Prdx1 (rPrdx1) causes ALI in *Prdx1*$^{-/-}$ mice.
- rPrdx1 induces IL-1β, IL-6, and TNF-α expression in primary macrophages.
- Circulating Prdx1 is a novel DAMP promoting ALI.